Electronic Supplementary Material (ESI) for ChemComm.

Electronic Supporting Information for

Highly Sensitive Detection of Cobalt Through Fluorescence Changes in β-Cyclodextrin-Bimane Complexes

Apurba Pramanik,[a] Sara Amer,[a] Flavio Grynzspan*[a] and Mindy Levine*[a]

TABLE OF CONTENTS

MATERIALS AND METHODS

All chemicals, including β-cyclodextrin, were purchased from commercial suppliers and used without further purification. All UV/Visible absorption spectra were recorded on a Varian Cary 50 Bio UV-Visible Spectrophotometer. Fluorescence spectra were recorded on a Varian Cary Eclipse Fluorescence Spectrophotometer. All FTIR spectra were obtained using KBr pellets and were recorded on a Perkin Elmer Spectrum One FT-IR spectrometer with KBr pellets. ^{1}H NMR spectra were obtained using a Bruker Avance III spectrophotometer operating at 400 MHz. All fluorescence spectra were integrated vs. wavenumber on the X-axis using OriginPro 2020. All curve fitting was done using OriginPro curve fitting options for both linear and non-linear curve fitting.

EXPERIMENTAL PROCEDURES

*Experimental Procedures for the Synthesis of Bimane **1***

syn-Bimane **1** was synthesized following the standard, solvent-free procedure reported by Neogi et. al.[1] In brief, we first synthesized 3,4-dimethyl-4-chloro-2-pyrazolin-5-one using solvent-free conditions.[1,2] Then 3,4-dimethyl-4-chloro-2-pyrazolin-5-one (0.2 g, 1.36 mmol, 1.0 equiv.) was melted via gentle heating and added to a scintillation vial containing $K_2CO_3 \cdot 1.5\ H_2O$ (0.945 mg, 5.71 mmol, 4.2 equiv.). The two components were rapidly mixed with a spatula at room temperature, and the progress of the reaction was monitored by TLC. The reaction reached completion after 15 minutes. After that, dichloromethane was added to the reaction mixture in five portions (ca. 15 mL each portion) and the combined organic extract was evaporated under reduced pressure. The reaction mixture was purified by column chromatography eluting with hexane/ethyl acetate (1:3). The desired 9,10-dioxa-syn-*(Me,Me)*bimane was isolated in 70% yield. ^{1}H NMR (D_2O, 400 MHz): δ = 1.77 (s, 3 H), 2.35 (s, 3 H) ppm. LC-MS: m/z calcd for $C_{10}H_{13}N_2O_2$: 193.09 [MH+]; found: 193.10.

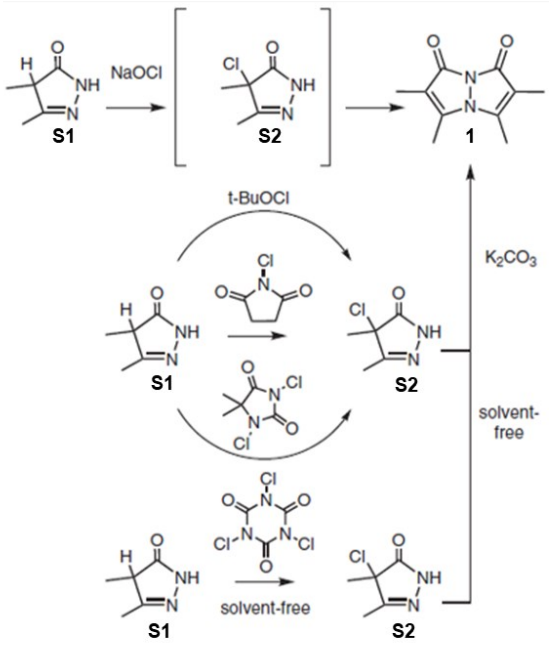

Figure S1. Schematic representation of the bimane synthesis

Experimental Procedures for UV-Vis Absorption Spectrometry

UV-Vis absorption spectroscopy was used in a number of situations: (a) to study the formation of an inclusion complex between bimane and β-cyclodextrin; (b) to investigate the detection of metal ions using bimane; and (c) to investigate the detection of metal ions using the complex formed between bimane and β-cyclodextrin. Procedures for each of these situations are detailed below.

(a) Formation of the inclusion complex between bimane and β-cyclodextrin

The formation of inclusion complex between bimane and β-cyclodextrin was investigated by measuring the UV-visible absorption spectra of bimane (200 - 700 nm) in aqueous solution at a concentration of 5.0×10^{-2} mM. The concentration of β-cyclodextrin in the aqueous solution varied from 0 mM β-cyclodextrin to 6.9×10^{-3} mM β-cyclodextrin.

(b) Investigation of the detection of metal ions using bimane

Ten metal chloride salts were investigated for their ability to induce changes in the UV-visible absorbance spectra of bimane: $BaCl_2$, $CaCl_2$, $CoCl_2$, $CuCl_2$, $HgCl_2$, $MgCl_2$, $MnCl_2$, $NiCl_2$, $SnCl_2$, and $ZnCl_2$. These experiments were conducted in double distilled water, with the bimane concentration held constant at 5.0×10^{-2} mM and 6.16×10^{-3} mM solutions of the various metal salts added. Because of the limited aqueous solubility of $SnCl_2$ and $ZnCl_2$, saturated solutions of the metal chloride salts were made and then filtered to remove insoluble particles. This filtered, saturated solution was used for further experimentation and analysis.

Further experimentation included the use of various concentrations of $CoCl_2$ in the presence of a constant bimane concentration of 5.0×10^{-2} mM. The concentration of $CoCl_2$ in these experiments ranged from 0 mM $CoCl_2$ (negative control) to 3.5×10^{-4} mM $CoCl_2$.

Additional experimentation included using the same concentration range of cobalt salts but with an acetate counterion ($Co(OAc)_2$) instead of chloride. The concentration of bimane was held constant at 5.0×10^{-2} mM and the concentration of $Co(OAc)_2$ ranged from 0 mM $Co(OAc)_2$ (negative control) to 3.5×10^{-4} mM $Co(OAc)_2$.

(c) Investigation of the detection of metal ions using the bimane - β-cyclodextrin complex

We followed the procedures described in part (b) but replaced the bimane fluorophore with the bimane-cyclodextrin complex. Concentrations of each component were identical to those listed in part (b), above.

Experimental Procedure for Fluorescence Spectroscopy

Fluorescence spectroscopy was used to investigate a variety of situations: (a) the formation of an inclusion complex between bimane and β-cyclodextrin; (b) the detection of metal salts via changes in the fluorescence emission of bimane; and (c) the detection of metal salts via changes in the fluorescence emission of the bimane: cyclodextrin complex. In all cases, the excitation of bimane occurred at 385 nm, and the excitation and emission slit widths were 2.5 nm and 5.0 nm, respectively. The procedures used in each of these situations are discussed in detail below:

(a) Complex formation between bimane and β-cyclodextrin

The concentration of bimane was held constant at 5.0×10^{-2} mM, and the concentration of β-cyclodextrin was varied from 0 mM β-cyclodextrin to 6.90×10^{-3} mM β-cyclodextrin. The fluorescence emission of the bimane in each case was recorded (excitation at 385 nm). Changes in the fluorescence emission of bimane were quantified by integrating the fluorescence emission vs. wavenumber on the X-axis (using OriginPro 2020), and the data were plotted using Benesi-Hildebrand and Stern-Volmer plots to determine binding and quenching constants, respectively.

(b) Metal ion detection using changes in bimane fluorescence emission

The concentration of bimane was held constant at 5.0×10^{-2} mM, and a variety of metal (II) chloride salts were added ($[MCl_2] = 6.16 \times 10^{-3}$ mM). The ten metal salts investigated were: $BaCl_2$, $CaCl_2$, $CoCl_2$, $CuCl_2$, $HgCl_2$, $MgCl_2$, $MnCl_2$, $NiCl_2$, $SnCl_2$, and $ZnCl_2$. Because of the limited aqueous solubility of $SnCl_2$ and $ZnCl_2$, saturated solutions of the metal chloride salts were made and then filtered to remove precipitates. This filtered, saturated solution was used for further experimentation and analysis. Changes in the fluorescence emission of bimane under these conditions were quantified by integrating the fluorescence emission vs. wavenumber on the X-axis using OriginPro 2020, and the data were plotted using Benesi-Hildebrand and Stern-Volmer plots to determine binding and quenching constants, respectively.

Increasing concentrations of cobalt (II) chloride were also monitored using fluorescence spectroscopy, with the concentration of bimane held constant at 5.0×10^{-2} mM. The concentration of $CoCl_2$ in these experiments ranged from 0 mM $CoCl_2$ (negative control) to 3.5×10^{-4} mM $CoCl_2$. Additional experimentation included using the same concentration range of cobalt salts but with a counterion of acetate ($Co(OAc)_2$) instead of chloride. The concentration of bimane was held constant at 5.0×10^{-2} mM and the concentration of $Co(OAc)_2$ ranged from 0 mM $Co(OAc)_2$ (negative control) to 3.5×10^{-4} mM $Co(OAc)_2$. In all cases, changes in the fluorescence emission of bimane under these conditions were quantified by integrating the fluorescence emission vs. wavenumber on the X-axis using OriginPro 2020, and the data were plotted using Benesi-Hildebrand and Stern-Volmer plots to determine binding and quenching constants, respectively.

The initial list of experiments was performed in double distilled water. A comparison of the results obtained in double distilled water to those obtained in unpurified tap water was also performed.

(c) Metal ion detection using changes in the fluorescence emission of the bimane-β-cyclodextrin complex

We followed the procedures described in part (b) but replaced the bimane fluorophore with the bimane-cyclodextrin complex. Concentrations of each component were identical to those listed in part (b), see above.

Experimental Procedure for Paper-Based Studies

Whatman #1 filter papers with dimensions of 5 cm x 0.75 cm were coated with a solution of bimane ([bimane] = 5.0 x 10^{-2} mM) and the complex of bimane in β-cyclodextrin ([complex] = 5.65 x 10^{-2} mM β-cyclodextrin and 5.0 x 10^{-2} mM bimane) by submerging the filter papers in solution for 30 minutes at room temperature. After thirty minutes, the papers were carefully removed from the solution using tweezers and were then placed on a Petri dish and allowed to dry overnight in an open-air environment. After that, 200 μL of an 0.1 M solution of a cobalt (II) salt (either $CoCl_2$ or $Co(OAc)_2$) were added and the paper was allowed to dry for 45 minutes at room temperature on the bench top. The dried papers were then visualized under a long wave TLC lamp (365 nm excitation) and the results of these studies are reported herein.

Experimental Procedure for ^{1}H NMR Titration Studies

15 mg of β-cyclodextrin and 15 mg of bimane **1** were each dissolved in 700 μL D_2O, and their ^{1}H NMR spectra were recorded. For the preparation of the β-cyclodextrin: bimane complex, 15 mg of a solid-state mixture (1:1 molar ratio β-cyclodextrin and bimane) was dissolved in 700 μL D_2O. For preparation of the bimane: cobalt complex, a 15 mg sample of a 1:1 molar ratio of the two components was dissolved in 700 μL D_2O. For preparation of the cobalt: bimane: β-cyclodextrin ternary mixture 15 mg of a 1:1:1 mixture of the three components was dissolved in 700 μL D_2O. All mixtures were vortexed for one hour in an Eppendorf tube prior to ^{1}H NMR analysis, and the resulting mixture was transferred to an ^{1}H NMR tube and analyzed.

Experimental Procedure for Solid-State FTIR Spectroscopy

A small amount of all samples (equimolar ratios for all mixtures) were ground by hand with a mortar and pestle for approximately 15 minutes. The resulting solid-state mixture was mixed with KBr salt and pellets were formed using the hydraulic pressure apparatus. To measure the solid-state FTIR spectra of the samples, first a background correction scan was conducted using a KBr pellet (without the sample). Following that, pellets made with the sample were placed in the FTIR spectrometer and the spectra were acquired. All data were saved as ASCII files and fitted using Microsoft Excel software.

Experimental Procedure for Limit of Detection Experiments

For Bimane

1. 100 µL of Bimane solution (0.1 mg/mL) in water was measured into a 15 mL glass vial. 2.40 mL Water were added. The vial was capped and left to stabilize for 48 hours.
2. The solution was transferred to a quartz cuvette and then excited at 385 nm and the fluorescence emission spectra was recorded from 400 to 700 nm. Each fluorescence measurement was repeated six times
3. 5.0 µL of the analyte solution $CoCl_2$ 0.1(M) in water was added to the cuvette and stirred thoroughly to ensure homogeneity. The solution was excited at the same wavelength (385 nm) and the emission was measured between 400 nm and 700 nm. Six repeat measurements were taken.
4. Step 2 was repeated four times for total addition volumes of 10 µL, 15 µL, 20 µL, and 25 µL of the analyte solution ($CoCl_2$). In all cases, the solution was excited at the same wavelength (385 nm) and the emission spectra from 400 to 700 nm was recorded six times.

For the Bimane-Cyclodextrin Complex

1. 100 µL of Bimane solution (0.1 mg/mL) in water was measured into a 15 mL glass vial. 2.00 mL of a 10 mM β-CD in water and 0.40 mL water were added. The vial was capped and left to stabilize for 48 hours.
2. The solution was transferred to a quartz cuvette and then excited at 385 nm and the fluorescence emission spectra was recorded from 400 to 700 nm. Each fluorescence measurement was repeated six times
3. 5.0 µL of the analyte solution $CoCl_2$ (0.1(M) in water was added to the cuvette and stirred thoroughly to ensure homogeneity. The solution was excited at the same wavelength (385 nm) and the emission was measured between 400 nm and 700 nm. Six repeat measurements were taken.
4. Step 2 was repeated four times for total addition volumes of 10 µL, 15 µL, 20 µL, and 25 µL of the analyte solution ($CoCl_2$). In all cases, the solution was excited at the same wavelength (385 nm) and the emission spectra from 400 to 700 nm was recorded six times.

For each case, a graph was plotted with integrated emission (vs. wavenumber) on the Y-axis and concentration of cobalt (II) chloride (in mM) on the X-axis, and an equation for the straight line was determined. The limit of the blank (LOD_{blank}) was defined according to the following equation:

$$LOD_{blank} = m_{blank} + 3(SD_{blank}) \quad \text{(Eq. S1)}$$

where m_{blank} is the mean of the blank integrations and SD_{blank} is the standard deviation of those measurements.

The LOD_{blank} was then entered into the equation determined from the plot of integrated emission vs concentration of cobalt (II) chloride, and the corresponding X-value was calculated. This value is the limit of detection of the analyte in mM in the system.

The limit of quantification of the blank (LOQ_{blank}) was calculated in a similar manner to the LOD. The limit of quantification of the blank is defined according to the following equation:

$$LOQ_{blank} = m_{blank} - 10(SD_{blank}). \quad \text{(Eq. S2)}$$

This value is then entered as the y-value from the derived equation, and the corresponding x-value was calculated. This is the value of the limit of quantification (LOQ) of the analyte for the system in mM.

Experimental Procedure for Relative Quantum Yield Experiments

The fluorescence spectra for calculating the quantum yield of bimane **1** and bimane 1 in a complex with β-cyclodextrin in water were recorded using a Varian Cary Eclipse fluorescence spectrophotometer equipped with a 10 mm pathlength quartz cuvette. The excitation slit width was 2.5 nm, the emission slit width was 2.5 nm, and the scan rate was 120 nm/min.

Quantum yields were calculated using the single point relative quantum yield method, according to Equation S3, below:[3]

$$(S3)\ \ \phi_{F(x)} = (\frac{n_x}{n_s})^2(\frac{A_s}{A_x})(\frac{I_{f(x)}}{I_{f(s)}})\phi_{F(s)}$$

where ϕ_F represents the fluorescence quantum yield, A represents the absorbance value, I_f represents the integration of the fluorescence band, and n represents the solvent refractive index. The subscripts s and x refer to the standard and unknown sample, respectively. In this work, the fluorescence quantum yield standards were solutions of 1,4-bis(5-phenyloxazol-2-yl)benzene (POPOP) in cyclohexane, with a reported relative quantum yield of 0.97.[4]

Experimental Procedure for ICP-MS Water Analysis

Standard solution preparation

In order to conduct these experiments, we prepared a 100 ppm standard solution for ICP-MS experiments, which contained Al, Ag, As, B, Ba, Be, Bi, Ca, Cd, Cs, Co, Cr, Cu, Fe, In, K, Li, Mg, Mn, Mo, Na, Ni, Nb, Pb, Rb, Sb, Se, Sr, Ti, Tl, V, U, Zn in 5% HNO_3 in water. We diluted this standard to 0.5 ppm, 1.0 ppm, and 5.0 ppm standard solutions for instrument standardization purposes.

Sample preparation:

For sample analysis, we prepared a solution of 1% HNO_3 in double distilled water and 1% HNO_3 in tap water separately and left each solution to sit for three hours. After the three hours, the solutions were filtered using 0.22 μm syringe filters and 10 mL of the filtrate solutions were used for the ICP-MS measurements.

We standardized the instrument with 0.5 ppm, 1.0 ppm and 5.0 ppm standard solutions in HNO_3. After that, we used the previously prepared 10 mL samples of 1% HNO_3 solution in double distilled water and 1% HNO_3 solution in tap water for metal detection. The data were recorded with Spectro Arcos (AMETEK, materials analysis division) spectrometer.

Experimental Procedure for Determination of Binding Constants via Supramolecular.org

Data was entered into BindFit, a program of Supramolecular.org, and was fit to a 1:1 binding complex using the UV algorithm fitter. All binding constants were determined using both integrated fluorescence emission values and intensity of the emission signal at various wavelengths, and the results are summarized in tabular format (*vide infra*).

SUMMARY TABLES

SUMMARY TABLES THAT ILLUSTRATE THE BINDING OF BIMANE IN β-CYCLODEXTRIN

Table S1. Changes in the integrated fluorescence emission of bimane in the presence of increasing concentrations of β-cyclodextrin[a]

[β-CD]	Integrated fluorescence emission[b]
0.00 mM	1.00 ± 0.0012
6.27 x 10^{-4} mM	0.96 ± 0.0014
1.26 x 10^{-3} mM	0.93 ± 0.0014
1.88 x 10^{-3} mM	0.89 ± 0.0007
2.51 x 10^{-3} mM	0.86 ± 0.0007
3.14 x 10^{-3} mM	0.84 ± 0.0007
3.76 x 10^{-3} mM	0.81 ± 0.0010
4.39 x 10^{-3} mM	0.78 ± 0.0001
5.02 x 10^{-3} mM	0.76 ± 0.0009
5.64 x 10^{-3} mM	0.73 ± 0.0003
6.27 x 10^{-3} mM	0.71 ± 0.0006
6.90 x 10^{-3} mM	0.69 ± 0.0001

[a] Bimane concentration was held constant at 5.0 x 10^{-2} mM. All reported results represent an average of at least two trials.

[b] Integrated fluorescence emission was normalized so that the highest integration value was set to 1.

Table S2. Percent decreases in the intensity of peaks at 230 nm, 255 nm, and 390 nm in the UV-visible absorption spectrum of bimane as a function of increasing concentrations of β-cyclodextrin[a]

[β-CD]	230 nm	255 nm	390 nm
0.00 mM	0%	0%	0%
6.27 x 10^{-4} mM	6.0 ± 0.02%	6.1 ± 0.10%	5.6 ± 0.03%
1.18 x 10^{-3} mM	10.5 ± 0.08%	11.2 ± 0.34%	10.8 ± 0.12%
1.67 x 10^{-3} mM	14.8 ± 0.07%	15.7 ± 0.33%	15.5 ± 0.02%
2.11 x 10^{-3} mM	18.8 ± 0.28%	19.6 ± 0.08%	19.5 ± 0.11%
2.51 x 10^{-3} mM	22.2 ± 0.21%	23.2 ± 0.29%	23.0 ± 0.05%
2.87 x 10^{-3} mM	25.3 ± 0.01%	26.2 ± 0.59%	26.4 ± 0.00%
3.19 x 10^{-3} mM	28.3 ± 0.08%	29.5 ± 0.23%	29.5 ± 0.06%
3.48 x 10^{-3} mM	30.7 ± 0.03%	32.2 ± 0.29%	32.3 ± 0.00%
3.75 x 10^{-3} mM	32.9 ± 0.15	34.4 ± 0.25	34.6 ± 0.08%
3.99 x 10^{-3} mM	35.2 ± 0.11	36.9 ± 0.19	37.1 ± 0.04%

4.21 x 10^{-3} mM	37.4 ± 0.02	39.0 ± 0.24	39.4 ± 0.02%

[a] Percent decreases were calculated according to the following equation:

Percent decrease = [(absorbance intensity of bimane at 0 mM of β-cyclodextrin) – (absorbance intensity of bimane at the specified β-cyclodextrin concentration)] / (absorbance intensity of bimane at 0 mM β-cyclodextrin) *100%

Table S3. Measurements of the binding constant of bimane in β-cyclodextrin (as determined via Benesi-Hildebrand plots) as well as the Stern-Volmer quenching constants[a]

$Log(K_a)$	K_a	Stern-Volmer quenching constant
5.81 ± 0.03	6.50 x 10^5 M^{-1}	6.48 x 10^5 M^{-1}

[a] All results represent an average of at least two trials.

SUMMARY TABLES THAT ILLUSTRATE THE INTERACTION OF A VARIETY OF METAL SALTS WITH BIMANE

Table S4. Summary of the fluorescence integration changes from treating a solution of bimane **1** with a variety of metal chloride salts[a]

Metal (II) chloride	Normalized fluorescence integration
none	1.00 ± 0.0000
Ba^{2+}	0.96 ± 0.0025
Ca^{2+}	0.97 ± 0.0021
Co^{2+}	0.62 ± 0.0010
Cu^{2+}	0.85 ± 0.0012
Hg^{2+}	0.95 ± 0.0010
Mg^{2+}	0.96 ± 0.0009
Mn^{2+}	0.94 ± 0.0008
Ni^{2+}	0.84 ± 0.0001
Sn^{2+}	0.77 ± 0.0002
Zn^{2+}	0.80 ± 0.0004

[a] [Bimane] = 5.0 x 10^{-2} mM; [metal salt] = 6.16 x 10^{-3} mM; all metal salts had chloride as a counterion; all reported results represent an average of three trials.

Table S5. Summary of the UV-visible spectral changes from treating a solution of bimane **1** with a variety of metal chloride salts[a]

Metal	Percent change at 390 nm[b]	Intensity changes at 510 nm[c]
none	0.00%	1.00 ± 0.00
Ba^{2+}	6.23 ± 0.12%	2.24 ± 0.81
Ca^{2+}	5.81 ± 0.05%	0.51 ± 0.28
Co^{2+}	5.46 ± 0.07%	490.15 ± 1.74
Cu^{2+}	4.28 ± 0.28%	61.68 ± 11.72
Hg^{2+}	5.69 ± 0.09%	-0.56 ± 0.43
Mg^{2+}	6.64 ± 0.14%	1.63 ± 0.73
Mn^{2+}	5.99 ± 0.03%	3.30 ± 1.71
Ni^{2+}	-7.65 ± 0.08%	6.72 ± 3.38
Sn^{2+}	-21.39 ± 0.83%	287.59 ± 7.27
Zn^{2+}	-26.90 ± 1.14%	289.20 ± 9.10

[a] [Bimane] = 5.0 x 10^{-2} mM; [metal salt] = 6.16 x 10^{-3} mM; all metal salts had chloride as a counterion; all reported results represent an average of three trials.

[b] Percent change was measured according to the following equation:

Percent change = (absorbance intensity in the absence of metal) – (absorbance intensity in the presence of metal) / (absorbance intensity in the absence of metal) * 100%

[c] For these results, the intensity of the UV-visible absorption peak at 510 nm in the presence of a metal chloride salt was divided by the intensity of the UV-visible absorption peak at 510 nm in the absence of a metal chloride salt

SUMMARY TABLES THAT ILLUSTRATE THE INTERACTION OF COBALT (II) CHLORIDE WITH BIMANE

Table S6. Changes in the integrated fluorescence emission of bimane in the presence of increasing concentrations of cobalt (II) chloride[a]

$[CoCl_2]$	Integrated fluorescence emission[b]
0.00 mM	1.00 ± 0.0012
3.23 x 10^{-5} mM	0.78 ± 0.0011
6.25 x 10^{-5} mM	0.62 ± 0.0007
9.10 x 10^{-5} mM	0.52 ± 0.0003
1.18 x 10^{-4} mM	0.44 ± 0.0000
1.43 x 10^{-4} mM	0.38 ± 0.0001
1.67 x 10^{-4} mM	0.34 ± 0.0004
1.88 x 10^{-4} mM	0.30 ± 0.0002
2.10 x 10^{-4} mM	0.27 ± 0.0004
2.31 x 10^{-4} mM	0.25 ± 0.0001
2.51 x 10^{-4} mM	0.23 ± 0.0003
2.71 x 10^{-4} mM	0.21 ± 0.0000
2.92 x 10^{-4} mM	0.19 ± 0.0006
3.12 x 10^{-4} mM	0.18 ± 0.0005
3.31 x 10^{-4} mM	0.18 ± 0.0001
3.51 x 10^{-4} mM	0.17 ± 0.0004

[a] Bimane concentration was held constant at 5.0 x 10^{-2} mM. All reported results represent an average of at least two trials.

[b] Integrated fluorescence emission was normalized so that the highest integration value was set to 1.

Table S7. Summary of how the changes in cobalt chloride concentration lead to changes in the UV-visible absorption spectra of bimane at higher concentrations of cobalt (II) chloride[a]

$[CoCl_2]$	% Change at 230 nm[b]	% Change at 255 nm[b]	% Change at 390 nm[b]	Intensity/ Initial intensity at 510 nm[c]
0.00 mM	0.00%	0.00%	0.00%	1.00
3.23 x 10^{-5} mM	0.01 ± 0.004%	0.02 ± 0.001%	0.02 ± 0.005%	11.84 ± 0.06
6.25 x 10^{-5} mM	0.03 ± 0.003%	0.04 ± 0.001%	0.04 ± 0.002%	22.60 ± 0.25
9.10 x 10^{-5} mM	0.05 ± 0.000%	0.05 ± 0.001%	0.06 ± 0.002%	33.11 ± 0.31
1.18 x 10^{-4} mM	0.06 ± 0.002%	0.07 ± 0.001%	0.08 ± 0.000%	42.42 ± 0.94
1.43 x 10^{-4} mM	0.08 ± 0.004%	0.09 ± 0.001%	0.10 ± 0.001%	51.16 ± 0.85
1.67 x 10^{-4} mM	0.09 ± 0.001%	0.11 ± 0.001%	0.12 ± 0.001%	59.46 ± 1.04

1.88 x 10^{-4} mM	0.11 ± 0.001%	0.13 ± 0.000%	0.14 ± 0.000%	67.18 ± 1.25
2.10 x 10^{-4} mM	0.13 ± 0.005%	0.14 ± 0.001%	0.15 ± 0.001%	75.27 ± 1.33
2.31 x 10^{-4} mM	0.15 ± 0.000%	0.16 ± 0.002%	0.17 ± 0.001%	82.54 ± 1.84
2.51 x 10^{-4} mM	0.16 ± 0.003%	0.17 ± 0.002%	0.19 ± 0.001%	89.64 ± 1.76
2.71 x 10^{-4} mM	0.18 ± 0.003%	0.19 ± 0.001%	0.21 ± 0.001%	95.78 ± 2.01
2.92 x 10^{-4} mM	0.19 ± 0.002%	0.20 ± 0.000%	0.22 ± 0.001%	102.05 ± 1.79
3.12 x 10^{-4} mM	0.20 ± 0.001%	0.22 ± 0.001%	0.23 ± 0.001%	107.85 ± 2.02
3.31 x 10^{-4} mM	0.21 ± 0.003%	0.23 ± 0.000%	0.25 ± 0.000%	113.41 ± 1.94
3.51 x 10^{-4} mM	0.23 ± 0.003%	0.25 ± 0.002%	0.26 ± 0.000%	118.66 ± 2.32

[a] Bimane concentration was held constant at 5.0 x 10^{-2} mM. All reported results represent an average of at least two trials.

[b] Percent change was measured according to the following equation:

Percent change = (absorbance intensity in the absence of metal) – (absorbance intensity in the presence of metal) / (absorbance intensity in the absence of metal) * 100%

[c] For these results, the intensity of the UV-visible absorption peak at 510 nm at a specified concentration of cobalt (II) chloride was divided by the intensity of the UV-visible absorption peak at 510 nm in the absence of cobalt (II) chloride

Table S8. Measurements of the binding constant of cobalt (II) chloride with bimane (as determined via Benesi-Hildebrand plots) as well as the Stern-Volmer quenching constants[a]

Log(K_a)	K_a	Stern-Volmer quenching constant
7.11 ±0.01	1.29 x 10^7 M^{-1}	1.18 x 10^7

[a] All results represent an average of at least two trials.

SUMMARY TABLES THAT ILLUSTRATE THE INTERACTION OF COBALT (II) ACETATE WITH BIMANE

Table S9. Changes in the integrated fluorescence emission of bimane in the presence of increasing concentrations of cobalt (II) acetate[a]

$[Co(OAc)_2]$	Integrated fluorescence emission[b]
0.00 mM	1.00 ± 0.0001
1.64 x 10^{-5} mM	0.86 ± 0.0007
3.23 x 10^{-5} mM	0.75 ± 0.0010
4.76 x 10^{-5} mM	0.67 ± 0.0004
6.25 x 10^{-5} mM	0.60 ± 0.0011
7.70 x 10^{-5} mM	0.55 ± 0.0002
9.10 x 10^{-5} mM	0.50 ± 0.0011
1.05 x 10^{-4} mM	0.46 ± 0.0005
1.18 x 10^{-4} mM	0.43 ± 0.0006
1.31 x 10^{-4} mM	0.40 ± 0.0003
1.43 x 10^{-4} mM	0.37 ± 0.0009
1.55 x 10^{-4} mM	0.35 ± 0.0003
1.67 x 10^{-4} mM	0.33 ± 0.0006

[a] Bimane concentration was held constant at 5.0 x 10^{-2} mM. All reported results represent an average of at least two trials.

[b] Integrated fluorescence emission was normalized so that the highest integration value was set to 1.

Table S10. Changes in the UV-visible absorption spectrum of bimane in the presence of increasing concentrations of cobalt (II) acetate[a]

$[Co(OAc)_2]$	230 nm[b]	255 nm[b]	390 nm[b]	510 nm[c]
0.00 mM	0.0%	0.0%	0.0%	1.0 ± 0.0
1.64 x 10^{-5} mM	0.4 ± 0.23%	1.4 ± 0.04%	1.5 ± 0.02%	29.0 ± 3.2
3.23 x 10^{-5} mM	0.2 ± 0.34%	2.7 ± 0.12%	2.7 ± 0.14%	56.9 ± 6.3
4.76 x 10^{-5} mM	0.7 ± 0.59%	4.1 ± 0.08%	4.1 ± 0.00%	84.5 ± 9.2
6.25 x 10^{-5} mM	0.6 ± 0.37%	5.3 ± 0.06%	5.3 ± 0.15%	111.0 ± 12.1
7.70 x 10^{-5} mM	0.7 ± 0.19%	6.7 ± 0.06%	6.4 ± 0.11%	137.3 ± 14.9
9.10 x 10^{-5} mM	0.7 ± 0.27%	7.9 ± 0.03%	7.7 ± 0.08%	163.4 ± 17.7
1.05 x 10^{-4} mM	0.8 ± 0.38%	8.9 ± 0.17%	8.3 ± 0.75%	192.6 ± 27.5
1.18 x 10^{-4} mM	0.8 ± 0.23%	10.3 ± 0.06%	10.0 ± 0.10%	212.2 ± 23.9
1.31 x 10^{-4} mM	1.3 ± 0.27%	11.3 ± 1.08%	11.1 ± 0.02%	236.8 ± 25.7
1.43 x 10^{-4} mM	0.9 ± 0.36%	12.5 ± 0.05%	12.2 ± 0.07%	259.5 ± 29.0

1.55×10^{-4} mM	0.9 ± 0.11%	13.5 ± 0.16%	13.1 ± 0.00%	282.5 ± 31.7
1.67×10^{-4} mM	0.7 ± 0.42%	14.6 ± 0.04%	14.1 ± 0.00%	304.5 ± 33.7

[a] Bimane concentration was held constant at 5.0×10^{-2} mM. All reported results represent an average of at least two trials.

[b] Percent decrease was calculated by subtracting the integrated fluorescence emission of bimane at 0 mM of cobalt (II) chloride by the integrated fluorescence emission of bimane at the specified concentration of cobalt (II) chloride and multiplying that value by 100%

[c] For these results, the intensity of the UV-visible absorption peak at 510 nm at a specified concentration of cobalt (II) chloride was divided by the intensity of the UV-visible absorption peak at 510 nm in the absence of cobalt (II) chloride

Table S11. Measurements of the binding constant of cobalt (II) acetate with bimane (as determined via Benesi-Hildebrand plots) as well as the Stern-Volmer quenching constants[a]

$Log(K_a)$	K_a	Stern-Volmer quenching constant
7.00 ± 0.01	$9.95 \times 10^{6}\ M^{-1}$	$1.23 \times 10^{7}\ M^{-1}$

[a] All results represent an average of at least two trials.

SUMMARY TABLES SHOWING THE INTERACTION OF DIFFERENT METAL SALTS WITH A BIMANE: β-CYCLODEXTRIN COMPLEX

Table S12. Summary of the fluorescence integration changes from treating a solution of bimane **1** with a variety of metal chloride salts[a]

Metal	Normalized fluorescence integration
none	1.00 ± 0.000
Ba^{2+}	0.95 ± 0.0002
Ca^{2+}	0.94 ± 0.0001
Co^{2+}	0.53 ± 0.0011
Cu^{2+}	0.83 ± 0.0031
Hg^{2+}	0.92 ± 0.0002
Mg^{2+}	0.94 ± 0.0003
Mn^{2+}	0.92 ± 0.0003
Ni^{2+}	0.82 ± 0.0013
Sn^{2+}	0.75 ± 0.0009
Zn^{2+}	0.78 ± 0.0003

a [Bimane] = 5.0 x 10^{-2} mM; [metal salt] = 6.16 x 10^{-3} mM; all metal salts had chloride as a counterion; all reported results represent an average of three trials.

Table S13. Summary of the UV-visible spectral changes from treating a solution of bimane **1** with a variety of metal salts[a]

Metal	Percent change at 390 nm[b]	Intensity/ Initial Intensity at 510 nm[c]
none	0.00%	1.00
Ba^{2+}	6.87 ± 0.00%	0.75 ± 0.000
Ca^{2+}	7.17 ± 0.00%	0.80 ± 0.000
Co^{2+}	-3.39 ± 0.62%	9.36 ± 0.058
Cu^{2+}	5.00 ± 1.76%	1.00 ± 0.206
Hg^{2+}	2.68 ± 0.00%	1.14 ± 0.000
Mg^{2+}	3.83 ± 0.00%	1.34 ± 0.000
Mn^{2+}	5.91 ± 0.19%	0.91 ± 0.060
Ni^{2+}	-24.48 ± 0.04%	0.90 ± 0.037
Sn^{2+}	-35.73 ±1.19%	3.97 ± 0.206
Zn^{2+}	-24.42 ± 0.45%	3.04 ± 0.082

[a] [Bimane] = 5.0 x 10^{-2} mM; [metal salt] = 6.16 x 10^{-3} mM; all metal salts had chloride as a counterion; all reported results represent an average of three trials.

[b] Percent change was measured according to the following equation:

Percent change = (absorbance intensity in the absence of metal) – (absorbance intensity in the presence of metal) / (absorbance intensity in the absence of metal) * 100%

[c] For these results, the intensity of the UV-visible absorption peak at 510 nm in the presence of a metal chloride salt was divided by the intensity of the UV-visible absorption peak at 510 nm in the absence of a metal chloride salt

SUMMARY TABLES THAT DEMONSTRATE THE INTERACTION OF COBALT (II) ACETATE WITH A BIMANE-β-CYCLODEXTRIN COMPLEX

Table S14. Summary of the UV-visible spectral changes from treating a solution of bimane **1** with cobalt (II) acetate[a]

$[Co(OAc)_2]$	230 nm[b]	255 nm[b]	390 nm[b]	510 nm[c]
0.00 mM	0.00%	0.00%	0.00%	1.00
1.64×10^{-5} mM	1.50 ± 0.18%	1.87 ± 0.14%	1.96 ± 0.62%	6.12 ± 0.79
3.23×10^{-5} mM	3.19 ± 0.21%	3.66 ± 0.20%	3.47 ± 0.54%	11.26 ± 1.47
4.76×10^{-5} mM	4.77 ± 0.14%	5.35 ± 0.07%	5.09 ± 0.30%	16.09 ± 1.99
6.25×10^{-5} mM	6.52 ± 0.20%	6.95 ± 0.06%	6.52 ± 0.46%	20.80 ± 2.66
7.70×10^{-5} mM	7.80 ± 0.30%	8.37 ± 0.02%	7.80 ± 0.42%	25.41 ± 3.16
9.10×10^{-5} mM	9.37 ± 0.02%	10.00 ± 0.11%	9.09 ± 0.42%	29.68 ± 3.61
1.05×10^{-4} mM	10.80 ± 0.15%	11.37 ± 0.07%	10.36 ± 0.54%	34.02 ± 4.18
1.18×10^{-4} mM	12.03 ± 0.10%	12.65 ± 0.13%	11.58 ± 0.57%	38.65 ± 4.14
1.31×10^{-4} mM	13.44 ± 0.16%	13.99 ± 0.00%	12.48 ± 0.12%	42.23 ± 5.20
1.43×10^{-4} mM	14.56 ± 0.10%	15.13 ± 0.11%	13.74 ± 0.31%	46.01 ± 5.67
1.55×10^{-4} mM	15.57 ± 0.02%	16.32 ± 0.04%	14.87 ± 0.36%	49.85 ± 6.26
1.67×10^{-4} mM	16.68 ±0.04%	17.51 ± 0.02%	15.77 ± 0.21%	53.42 ± 6.71

[a] Bimane concentration was held constant at 5.0×10^{-2} mM. All reported results represent an average of at least two trials.

[b] Percent change was measured according to the following equation:

Percent change = (absorbance intensity in the absence of metal) – (absorbance intensity in the presence of metal) / (absorbance intensity in the absence of metal) * 100%

[c] For these results, the intensity of the UV-visible absorption peak at 510 nm at a specified concentration of cobalt (II) chloride was divided by the intensity of the UV-visible absorption peak at 510 nm in the absence of cobalt (II) chloride

Table S15. Changes in the integrated fluorescence emission of the bimane-β-cyclodextrin complex in the presence of increasing concentrations of cobalt (II) acetate[a]

$[Co(OAc)_2]$	Integrated fluorescence emission[b]
0.00 mM	1.00 ± 0.0004
1.64×10^{-5} mM	0.84 ± 0.0012
3.23×10^{-5} mM	0.72 ± 0.0002
4.76×10^{-5} mM	0.63 ± 0.0003
6.25×10^{-5} mM	0.56 ± 0.0001
7.70×10^{-5} mM	0.50 ± 0.0025
9.10×10^{-5} mM	0.45 ± 0.0002

1.05 x 10^{-4} mM	0.41 ± 0.0002
1.18 x 10^{-4} mM	0.38 ± 0.0000
1.31 x 10^{-4} mM	0.35 ± 0.0001
1.43 x 10^{-4} mM	0.32 ± 0.0007
1.55 x 10^{-4} mM	0.30 ± 0.0002
1.67 x 10^{-4} mM	0.28 ± 0.0007

[a] Bimane concentration was held constant at 5.0 x 10^{-2} mM. All reported results represent an average of at least two trials.

[b] Integrated fluorescence emission was normalized so that the highest integration value was set to 1.

[c] Percent decrease was calculated by subtracting the integrated fluorescence emission of bimane at 0 mM of cobalt (II) acetate by the integrated fluorescence emission of the bimane-β-cyclodextrin complex at the specified concentration of cobalt (II) acetate and multiplying that value by 100%

Table S16. Measurements of the binding constant of cobalt (II) acetate with the bimane-β-cyclodextrin complex (as determined via Benesi-Hildebrand plots) as well as the Stern-Volmer quenching constants[a]

Log(K_a)	K_a	Stern-Volmer quenching constant
7.05 ± 0.0045	1.13 x 10^7 M^{-1}	1.72 x 10^7 M

[a] All results represent an average of at least two trials.

SUMMARY TABLES THAT ILLUSTRATE THE INTERACTION OF COBALT (II) CHLORIDE WITH THE BIMANE-β-CYCLODEXTRIN COMPLEX

Table S17. Changes in the integrated fluorescence emission of the bimane-β-cyclodextrin complex in the presence of increasing concentrations of cobalt (II) chloride[a]

[$CoCl_2$]	Integrated fluorescence emission[b]
0.00 mM	1.00 ± 0.001
3.23 x 10^{-5} mM	0.73 ± 0.000
6.25 x 10^{-5} mM	0.57 ± 0.001
9.10 x 10^{-5} mM	0.47 ± 0.001
1.18 x 10^{-4} mM	0.39 ± 0.002
1.43 x 10^{-4} mM	0.34 ± 0.001
1.67 x 10^{-4} mM	0.30 ± 0.002
1.88 x 10^{-4} mM	0.26 ± 0.000
2.10 x 10^{-4} mM	0.24 ± 0.002
2.31 x 10^{-4} mM	0.21 ± 0.000
2.51 x 10^{-4} mM	0.19 ± 0.001
2.71 x 10^{-4} mM	0.18 ± 0.000
2.92 x 10^{-4} mM	0.17 ± 0.001
3.12 x 10^{-4} mM	0.16 ± 0.001

[a] Bimane concentration was held constant at 5.0 x 10^{-2} mM. All reported results represent an average of at least two trials.

[b] Integrated fluorescence emission was normalized so that the highest integration value was set to 1.

Table S18. Changes in the UV-visible absorption spectrum of the bimane-β-cyclodextrin complex in the presence of increasing concentrations of cobalt (II) chloride[a]

[$CoCl_2$]	% Change at 230 nm[b]	% Change at 255 nm[b]	% Change at 390 nm[b]	Intensity/ Initial intensity at 510 nm[c]
0.00 mM	0.00%	0.00%	0.00%	1.00
3.23 x 10^{-5} mM	3.34 ± 0.00%	3.66 ± 0.20%	3.47 ± 0.54%	11.26 ± 1.47
6.25 x 10^{-5} mM	6.38 ± 0.00%	6.95 ± 0.06%	6.52 ± 0.46%	20.80 ± 2.66
9.10 x 10^{-5} mM	9.36 ± 0.00%	10.00 ± 0.11%	9.09 ± 0.42%	29.68 ± 3.61
1.18 x 10^{-4} mM	11.96 ± 0.00%	12.65 ± 0.13%	11.58 ± 0.57%	38.65 ± 4.14
1.43 x 10^{-4} mM	14.63 ± 0.00%	15.13 ± 0.11%	13.74 ± 0.31%	46.01 ± 5.67
1.67 x 10^{-4} mM	16.66 ± 0.00%	17.51 ± 0.02%	15.77 ± 0.21%	53.42 ± 6.71
1.88 x 10^{-4} mM	18.90 ± 0.00%	19.73 ± 0.02%	17.83 ± 0.25%	60.56 ± 7.62
2.10 x 10^{-4} mM	20.72 ± 0.00%	21.89 ± 0.08%	19.62 ± 0.31%	66.98 ± 8.27

2.31 x 10^{-4} mM	22.92 ± 0.00%	23.95 ± 0.07%	21.67 ± 0.23%	73.33 ± 9.11
2.51 x 10^{-4} mM	24.70 ± 0.00%	25.67 ± 0.02%	23.16 ± 0.15%	79.01 ± 9.77
2.71 x 10^{-4} mM	26.14 ± 0.00%	27.37 ± 0.08%	24.76 ± 0.36%	84.61 ± 10.52
2.92 x 10^{-4} mM	25.58 ± 0.00%	27.09 ± 0.03%	24.44 ± 0.31%	90.60 ± 11.18
3.12 x 10^{-4} mM	26.57 ± 0.00%	28.19 ± 0.03%	25.57 ± 0.17%	95.77 ± 11.64

[a] Bimane concentration was held constant at 5.0 x 10^{-2} mM. All reported results represent an average of at least two trials.

[b] Percent change was measured according to the following equation:

Percent change = (absorbance intensity in the absence of metal) – (absorbance intensity in the presence of metal) / (absorbance intensity in the absence of metal) * 100%

[c] For these results, the intensity of the UV-visible absorption peak at 510 nm at a specified concentration of cobalt (II) chloride was divided by the intensity of the UV-visible absorption peak at 510 nm in the absence of cobalt (II) chloride

Table S19. Measurements of the binding constant of cobalt (II) chloride with the bimane-β-cyclodextrin complex (as determined via Benesi-Hildebrand plots) as well as the Stern-Volmer quenching constants[a]

Log(K_a)	K_a	Stern-Volmer quenching constant
7.04 ± 0.01	1.08 x 10^7 M^{-1}	1.43 x 10^7 M

[a] All results represent an average of at least two trials.

Information that shows the upper limit of concentration for $CoCl_2$ using the bimane-β-cyclodextrin complex:

Table S19. Summary of how the changes in cobalt (II) chloride concentration lead to changes in the fluorescence emission spectra of the bimane-β-cyclodextrin complex and eventual leveling off of the signal above 2.71 x 10^{-4} mM of $CoCl_2$

[$CoCl_2$]	Integrated fluorescence emission[b]
0.00 mM	1.00 ± 0.00
3.23 x 10^{-5} mM	0.73 ± 0.0003
6.25 x 10^{-5} mM	0.57 ± 0.0009
9.10 x 10^{-5} mM	0.47 ± 0.0012
1.18 x 10^{-4} mM	0.39 ± 0.0017
1.43 x 10^{-4} mM	0.34 ± 0.0013
1.67 x 10^{-4} mM	0.30 ± 0.0017
1.88 x 10^{-4} mM	0.26 ± 0.0000
2.10 x 10^{-4} mM	0.24 ± 0.0017
2.31 x 10^{-4} mM	0.21 ± 0.0000
2.51 x 10^{-4} mM	0.19 ± 0.0012
2.71 x 10^{-4} mM	0.18 ± 0.0005

2.92 x 10^{-4} mM	0.17 ± 0.0007
3.12 x 10^{-4} mM	0.16 ± 0.0009

[a] Bimane concentration was held constant at 5.0 x 10^{-2} mM. All reported results represent an average of at least two trials.

[b] Integrated fluorescence emission was normalized so that the highest integration value was set to 1.

Table S20. Summary of how the changes in cobalt chloride concentration lead to changes in the UV-visible absorption spectra of the bimane-β-cyclodextrin complex and eventual leveling off of the signal above 2.71 x 10^{-4} mM of $CoCl_2$[a]

[$CoCl_2$]	% Change at 230 nm[b]	% Change at 255 nm[b]	% Change at 390 nm[b]	Intensity/ Initial intensity at 510 nm[c]
0.00 mM	0.00%	0.00%	0.00%	1.00%
3.23 x 10^{-5} mM	3.19 ± 0.22%	3.66 ± 0.20%	3.47 ± 0.54%	11.26 ± 1.47%
6.25 x 10^{-5} mM	6.52 ± 0.20%	6.95 ± 0.06%	6.52 ± 0.46%	20.80 ± 2.66%
9.10 x 10^{-5} mM	9.37 ± 0.02%	10.00 ± 0.11%	9.09 ± 0.42%	29.68 ± 3.61%
1.18 x 10^{-4} mM	12.03 ± 0.10%	12.65 ± 0.13%	11.58 ± 0.57%	38.65 ± 4.14%
1.43 x 10^{-4} mM	14.56 ± 0.10%	15.13 ± 0.11%	13.74 ± 0.31%	46.01 ± 5.67%
1.67 x 10^{-4} mM	16.68 ± 0.04%	17.51 ± 0.02%	15.77 ± 0.21%	53.42 ± 6.71%
1.88 x 10^{-4} mM	18.94 ± 0.06%	19.73 ± 0.02%	17.83 ± 0.25%	60.56 ± 7.62%
2.10 x 10^{-4} mM	20.93 ± 0.29%	21.89 ± 0.08%	19.62 ± 0.31%	66.98 ± 8.27%
2.31 x 10^{-4} mM	22.94 ± 0.03%	23.95 ± 0.07%	21.67 ± 0.23%	73.33 ± 9.11%
2.51 x 10^{-4} mM	24.52 ± 0.26%	25.67 ± 0.02%	23.16 ± 0.15%	79.01 ± 9.77%
2.71 x 10^{-4} mM	26.23 ± 0.13%	27.37 ± 0.08%	24.76 ± 0.36%	84.61 ± 10.52%
2.92 x 10^{-4} mM	25.45 ± 0.18%	27.09 ± 0.03%	24.44 ± 0.31%	90.60 ± 11.18%
3.12 x 10^{-4} mM	26.59 ± 0.02%	28.19 ± 0.03%	25.57 ± 0.17%	95.77 ± 11.64%

[a] Bimane concentration was held constant at 5.0 x 10^{-2} mM. All reported results represent an average of at least two trials.

[b] Percent change was measured according to the following equation:

Percent change = (absorbance intensity in the absence of metal) – (absorbance intensity in the presence of metal) / (absorbance intensity in the absence of metal) * 100%

[c] For these results, the intensity of the UV-visible absorption peak at 510 nm at a specified concentration of cobalt (II) chloride was divided by the intensity of the UV-visible absorption peak at 510 nm in the absence of cobalt (II) chloride

SUMMARY TABLES ILLUSTRATING EXPERIMENTS IN TAP WATER

Bimane response to cobalt (II) chloride in tap water

Table S21. Changes in the integrated fluorescence emission of bimane in the presence of increasing concentrations of cobalt (II) chloride in tap water[a]

[$CoCl_2$]	Integrated fluorescence emission[b]
0.00 mM	1.00 ± 0.001
1.64 x 10^{-5} mM	0.87 ± 0.002
3.23 x 10^{-5} mM	0.76 ± 0.002
4.76 x 10^{-5} mM	0.68 ± 0.001
6.25 x 10^{-5} mM	0.61 ± 0.001
7.70 x 10^{-5} mM	0.56 ± 0.000
9.10 x 10^{-5} mM	0.50 ± 0.000
1.05 x 10^{-4} mM	0.46 ± 0.000
1.18 x 10^{-4} mM	0.43 ± 0.000
1.31 x 10^{-4} mM	0.40 ± 0.000
1.43 x 10^{-4} mM	0.37 ± 0.000
1.55 x 10^{-4} mM	0.34 ± 0.000
1.67 x 10^{-4} mM	0.32 ± 0.000

[a] Bimane concentration was held constant at 5.0 x 10^{-2} mM. All reported results represent an average of at least two trials.

[b] Integrated fluorescence emission was normalized so that the highest integration value was set to 1.

Table S22. Changes in the UV-visible absorption spectrum of bimane in the presence of increasing concentrations of cobalt (II) chloride in tap water[a]

[$CoCl_2$]	230 nm[b]	255 nm[b]	390 nm[b]
0.00 mM	0.00%	0.00%	0.00%
1.64 x 10^{-5} mM	-0.61 ± 0.41%	0.01 ± 0.05%	0.11 ± 0.15%
3.23 x 10^{-5} mM	-0.46 ± 0.16%	0.53 ± 0.01%	0.67 ± 0.21%
4.76 x 10^{-5} mM	-0.14 ± 0.50%	0.94 ± 0.10%	0.74 ± 0.32%
6.25 x 10^{-5} mM	-0.26 ± 0.82%	1.49 ± 0.17%	0.94 ± 0.15%
7.70 x 10^{-5} mM	0.74 ± 0.21%	2.13 ± 0.15%	1.68 ± 0.04%
9.10 x 10^{-5} mM	1.88 ± 0.61%	2.98 ± 0.21%	2.19 ± 0.67%
1.05 x 10^{-4} mM	2.27 ± 0.16%	3.85 ± 0.17%	2.65 ± 0.86%
1.18 x 10^{-4} mM	3.21 ± 0.17%	4.85 ± 0.23%	3.62 ± 0.56%
1.31 x 10^{-4} mM	4.49 ± 0.71%	6.00 ± 0.09%	4.19 ± 0.27%

1.43 x 10^{-4} mM	5.32 ± 0.92%	6.88 ± 0.12%	5.01 ± 0.30%
1.55 x 10^{-4} mM	6.81 ± 0.16%	8.37 ± 0.07%	5.92 ± 0.42%
1.67 x 10^{-4} mM	8.43 ± 0.45%	9.72 ± 0.08%	7.48 ± 0.15%

[a] Bimane concentration was held constant at 5.0 x 10^{-2} mM. All reported results represent an average of at least two trials.

[b] Percent change was measured according to the following equation:

Percent change = (absorbance intensity in the absence of metal) – (absorbance intensity in the presence of metal) / (absorbance intensity in the absence of metal) * 100%

Response of the bimane:β- cyclodextrin complex to cobalt (II) chloride in tap water

Table S23. Changes in the integrated fluorescence emission of the bimane: β-cyclodextrin complex in the presence of increasing concentrations of cobalt (II) chloride in tap water[a]

[$CoCl_2$]	Integrated fluorescence emission[b]
0.00 mM	1.00 ± 0.001
1.64 x 10^{-5} mM	0.83 ± 0.001
3.23 x 10^{-5} mM	0.71 ± 0.000
4.76 x 10^{-5} mM	0.62 ± 0.000
6.25 x 10^{-5} mM	0.55 ± 0.000
7.70 x 10^{-5} mM	0.48 ± 0.000
9.10 x 10^{-5} mM	0.44 ± 0.000
1.05 x 10^{-4} mM	0.40 ± 0.00
1.18 x 10^{-4} mM	0.36 ± 0.001
1.31 x 10^{-4} mM	0.33 ± 0.000
1.43 x 10^{-4} mM	0.31 ± 0.000
1.55 x 10^{-4} mM	0.29 ± 0.000
1.67 x 10^{-4} mM	0.27 ± 0.000

[a] Bimane concentration was held constant at 5.0 x 10^{-2} mM. All reported results represent an average of at least two trials.

[b] Integrated fluorescence emission was normalized so that the highest integration value was set to 1.

Table S24. Changes in the UV-visible absorption spectrum of the bimane: β-cyclodextrin complex in the presence of increasing concentrations of cobalt (II) chloride in tap water[a]

[$CoCl_2$]	230 nm[b]	255 nm[b]	390 nm[b]
0.00 mM	0.00%	0.00%	0.00%
1.64 x 10^{-5} mM	-1.04 ± 0.93%	1.34 ± 3.44%	1.02 ± 1.19%
3.23 x 10^{-5} mM	0.16 ± 1.93%	3.67 ± 3.93%	4.31 ± 2.73%
4.76 x 10^{-5} mM	0.97 ± 0.85%	4.50 ± 2.52%	3.57 ± 1.02%

6.25 x 10^{-5} mM	1.50 ± 0.67%	5.96 ± 2.01%	5.02 ± 0.63%
7.70 x 10^{-5} mM	1.57 ± 1.08%	6.28 ± 2.74%	4.67 ± 1.30%
9.10 x 10^{-5} mM	1.99 ± 0.74%	7.07 ± 2.43%	5.36 ± 0.60%
1.05 x 10^{-4} mM	3.22 ± 0.74%	8.35 ± 2.53%	5.81 ± 1.67%
1.18 x 10^{-4} mM	3.49 ± 1.44%	8.99 ± 3.00%	6.43 ± 1.29%
1.31 x 10^{-4} mM	5.41 ± 0.84%	11.22 ± 2.73%	9.67 ± 3.17%
1.43 x 10^{-4} mM	5.91 ± 1.21%	12.42 ± 3.08%	10.62 ± 4.06%
1.55 x 10^{-4} mM	6.36 ± 0.85%	13.60 ± 1.90%	11.32 ± 0.45%
1.67 x 10^{-4} mM	7.21 ± 1.01%	14.30 ± 2.62%	12.53 ± 0.63%

[a] Bimane concentration was held constant at 5.0 x 10^{-2} mM. All reported results represent an average of at least two trials.

[b] Percent change was measured according to the following equation:

Percent change = (absorbance intensity in the absence of metal) – (absorbance intensity in the presence of metal) / (absorbance intensity in the absence of metal) * 100%

SUMMARY TABLE FOR LIMIT OF DETECTION STUDIES

Table S25. Table summarizing the limit of detection and limit of quantification for cobalt (II) chloride in double distilled water using changes in the bimane fluorescence emission as well as changes in the emission of the bimane: β-cyclodextrin complex[a]

	Bimane	Bimane: β-Cyclodextrin Complex
Limit of Detection	0.88 ± 0.02 nM	0.60 ± 0.05 nM
Limit of Quantification	1.32 ± 0.08 nM	1.00 ± 0.15 nM
Linear Equation	y = (-7E10)x + (1E6)	y = (-8E10)x + (1E6)
R^2 value	0.9922	0.9896

[a] Limits of detection and limits of quantification were calculated following the procedures detailed above (*vide supra*)

Table S26. Table summarizing the limit of detection and limit of quantification for cobalt (II) chloride in tap water using changes in the bimane fluorescence emission as well as changes in the emission of the bimane: β-cyclodextrin complex[a]

	Bimane	Bimane: β-Cyclodextrin Complex
Limit of Detection	1.50 ± 0.01	0.99 ± 0.004
Limit of Quantification	1.72 ± 0.02	1.04 ± 0.015
Linear Equation	y = (-8E10)x + (1E6)	y = (-1E11)x + (1E6)
R^2 value	0.9832	0.9957

[a] Limits of detection and limits of quantification were calculated following the procedures detailed above (*vide supra*)

SUMMARY TABLES FOR SOLID-STATE DETECTION

Table S27. Changes in quantitative image values upon exposure of solid-state sensors to cobalt (II) chloride[a]

	Δ saturation	Δ luminescence	Δ blue
Filter paper coated in **1**: β-cyclodextrin complex	13.3 ± 0.8	32.5 ± 0.7	75.6 ± 0.7
Filter paper coated in compound **1**	0.3 ± 0.1	26.5 ± 0.4	56.1 ± 0.6
% improvement in complex[b]	4333%	22.6%	34.8%

[a] Δ values in all cases were calculated as the absolute value of the difference between the value obtained from the filter paper exposed to cobalt (II) chloride and the value obtained from the filter paper that had not been exposed to cobalt (II) chloride. All values represent an average of 10 data points taken randomly from the images and quantified using Microsoft Paint.

[b] % improvement in complex was calculated according to the following equation:

$(Response_{complex} - Response_{bimane})/ Response_{bimane}$ x 100%,

where $Response_{bimane}$ refers to the quantitative response in the presence of bimane **1** alone and $Response_{complex}$ refers to the quantitative response determined using the bimane **1**-β-cyclodextrin complex.

SUMMARY TABLES FOR [1]H NMR TITRATION STUDIES

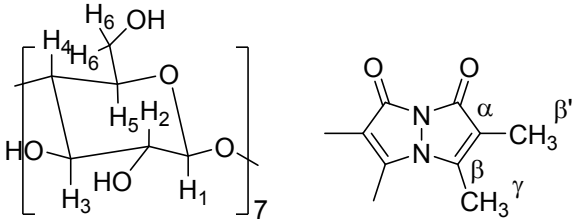

Figure S2. Illustration of the structures of bimane **1** and β-cyclodextrin with the protons investigated clearly delineated

Table S28. [1]H NMR chemical shifts of β-cyclodextrin protons without bimane ("free") and in the presence of bimane in a 1:1 molar ratio ("in complex") in D_2O[a]

Proton	Free β-cyclodextrin (ppm)	β-cyclodextrin in complex (ppm)	Δδ (ppm)
H1	5.118	5.120	0.002
H2	3.701	3.703	0.002
H3	**4.009**	**3.998**	**-0.011**
H4	3.624	3.628	0.004
H5	**3.898**	**3.890**	**-0.008**
H6ab	3.921	3.922	0.001

[a] Values were measured on a 400 MHz NMR spectrometer using D_2O as a solvent

Table S29. [1]H NMR chemical shifts of bimane protons without β-cyclodextrin ("free") in the presence of a 1:1 molar ratio of β-cyclodextrin ("in complex") in D_2O[a]

Proton	Free bimane (ppm)	Bimane in complex (ppm)	Δδ (ppm)
$^{\beta'}CH_3$	2.352	2.363	0.011
$^{\gamma}CH_3$	1.769	1.778	0.011

[a] Values were measured on a 400 MHz NMR spectrometer using D_2O as a solvent

Table S30. [1]H NMR chemical shifts of bimane protons without any additives ("free") and in the presence of a mixture of β-cyclodextrin and cobalt (II) chloride (1:1:1 molar ratio) in D_2O ("in complex")[a]

Proton	Free bimane (ppm)	Bimane in complex with cobalt (II) chloride (ppm)	Δδ (ppm)
$^{\beta'}CH_3$	2.352	1.627	-0.725
$^{\gamma}CH_3$	1.769	1.042	-0.727

[a] Values were measured on a 400 MHz NMR spectrometer using D_2O as a solvent

Table S31. [1]H NMR chemical shifts of bimane protons without any additives ("free") and in the presence of cobalt (II) chloride (1:1 molar ratio) in D_2O[a]

Proton	Free bimane (ppm)	Bimane with cobalt (II) chloride (ppm)	Δδ (ppm)
$^{\beta'}CH_3$	2.352	2.066	-0.286
$^{\gamma}CH_3$	1.769	1.483	-0.286

[a] Values were measured on a 400 MHz NMR spectrometer using D_2O as a solvent

Summary Tables for Relative Quantum Yield Experiments

Table S32. Relative quantum yield of compound **1** measured under a variety of experimental conditions[a]

Solvent	Experimental conditions	Relative quantum yield
100% dioxane	[**1**] = 10 μM	0.83
72% dioxane: 28% water	[**1**] = 10 μM	0.84
100% water	[**1**] = 10 μM	0.486
100% water	**1** in complex with β-CD	0.493

[a] All relative quantum yields were measured relative to the standard POPOP (1, 4-bis(5-phenyloxazole-2-yl)benzene) and displayed good agreement with literature-reported values[5]

Summary Table for ICP-MS Water Analysis

Table S33. ICP-MS Analytical Results for the Metal Ion Content in Double Distilled Water and Tap Water, with concentration results reported in ppm units.

Metals	Double distilled water (DDW)	Tap Water
Ag	<0.003	<0.003
Al	<0.021	<0.044
As	<0.007	<0.007
Ba	<0.000	<0.030
Be	<0.000	<0.000
Ca	<0.040	>21.037
Cd	<0.001	<0.001
Co	<0.001	<0.001
Cr	<0.000	<0.000
Cu	<0.002	<0.002
Fe	<0.001	<0.001
In	<0.046	<0.046
Li	<0.004	0.006
Mg	<0.000	>22.690
Mn	<0.000	<0.000
Mo	<0.009	<0.002
Na	<0.044	>48.820
Ni	<0.002	<0.002
Pb	<0.009	<0.009
Sb	0.033	<0.019
Se	<0.023	<0.023
Sr	<0.000	<0.609
Ti	<0.000	<0.000
Tl	<0.004	<0.004
U	<0.103	<0.103
V	<0.001	<0.001
Zn	0.003	0.067

Summary Table for Binding Constants Determined via Supramolecular.org

Table S34. Summary of binding constants obtained via fitting to a BindFit 1:1 complex[a]

Host	Guest	Binding constant via fluorescence integration	Binding constant via fluorescence intensity
1	β-cyclodextrin	2.2 x 10^4 M^{-1} (8.6% error)	2.2 x 10^4 M^{-1} (3.75% error)
1	cobalt (II) chloride	2.0 x 10^4 M^{-1} (19% error)	2.0 x 10^4 M^{-1} (8.1% error)
1: β-CD complex	cobalt (II) chloride	2.0 x 10^4 M^{-1} (23% error)	2.0 x 10^4 M^{-1} (9.8% error)

[a] All data was determined using the BindFit tab on supramolecular.org, using the 1:1 UV data algorithm, with constants determined using both fluorescence integration values as well as fluorescence intensity values at 4 wavelengths throughout the emission spectra.

Summary Tables for Metal Competition Studies to Determine Cobalt Selectivity

Table S35. Changes in the fluorescence emission of bimane **1** and of a bimane: β-cyclodextrin complex upon introduction of cobalt (II) chloride in the presence and absence of other metal additives[a]

Metal Cation Identity	Fluorescence Response of Bimane	Fluorescence Response of Bimane: β-Cyclodextrin Complex
No metal	100.0 ± 0.0 %	100.0 ± 0.0%
Ba (II) and Co (II)	62.1 ± 0.1 %	54.6 ± 0.0%
Ca (II) and Co (II)	62.3 ± 0.1 %	56.0 ± 0.1%
Co (II)	61.5 ± 0.1 %	54.8 ± 0.1%
Cu (II) and Co (II)	54.9 ± 0.1 %	50.1 ± 0.1%
Hg (II) and Co (II)	61.4 ± 0.0 %	53.4 ± 0.0%
Mg (II) and Co (II)	62.9 ± 0.0 %	55.3 ± 0.0%
Mn (II) and Co (II)	62.4 ± 0.1 %	54.6 ± 0.1%
Ni (II) and Co (II)	58.5 ± 0.1 %	52.4 ± 0.1%
Sn (II) and Co (II)	52.7 ± 0.3 %	48.3 ± 0.1%
Zn (II) and Co (II)	53.2 ± 0.0 %	47.5 ± 0.1%

[a] Values are measured as percentages of normalized integrated emission, with the maximum integrated emission set to 100%. Results reported herein represent the average of at least two trials.

Table S36. Summary of the UV-visible spectral changes of bimane **1** and of a bimane: β-cyclodextrin complex upon introduction of cobalt (II) chloride in the presence and absence of other metal additives[a]

Metal	Intensity Changes of Bimane	Intensity Changes of a Bimane: β-Cyclodextrin Complex
none	1.1 ± 0.1	1.0 ± 0.0
Ba (II) and Co (II)	220.3 ± 10.6	7.7 ± 0.2
Ca (II) and Co (II)	231.3 ± 4.4	6.1 ± 0.2
Co (II)	226.3 ± 2.9	6.7 ± 0.2
Cu (II) and Co (II)	275.7 ± 0.0	6.4 ± 0.2
Hg (II) and Co (II)	189.8 ± 0.8	7.9 ± 0.2
Mg (II) and Co (II)	199.6 ± 1.0	7.0 ± 0.2
Mn (II) and Co (II)	176.9 ± 4.3	6.6 ± 0.2
Ni (II) and Co (II)	206.0 ± 6.2	6.5 ± 0.2
Sn (II) and Co (II)	177.3 ± 0.4	6.1 ± 0.2
Zn (II) and Co (II)	201.3 ± 2.6	6.1 ± 0.2

[a] [Bimane] = 5.0 x 10^{-2} mM; [metal salt] = 6.16 x 10^{-3} mM; all metal salts had chloride as a counterion; all reported results represent an average of three trials.

[b] The intensity of the UV-visible absorption peak at 510 nm in the presence of a metal chloride salt was divided by the intensity of the UV-visible absorption peak at 510 nm in the absence of a metal chloride salt

SUMMARY FIGURES

*SUMMARY FIGURES FOR THE SYNTHESIS OF BIMANE **1***

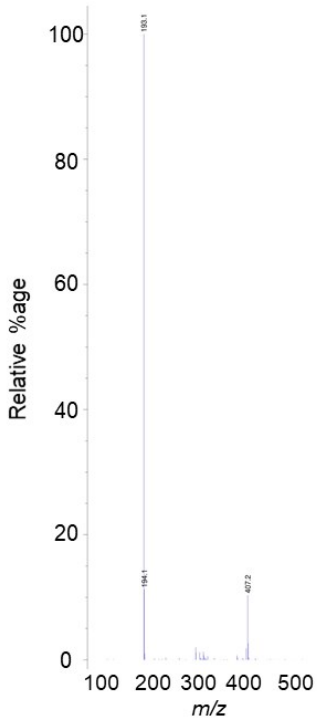

Figure S3. Results of the mass spectral analysis of the structure of bimane **1**.

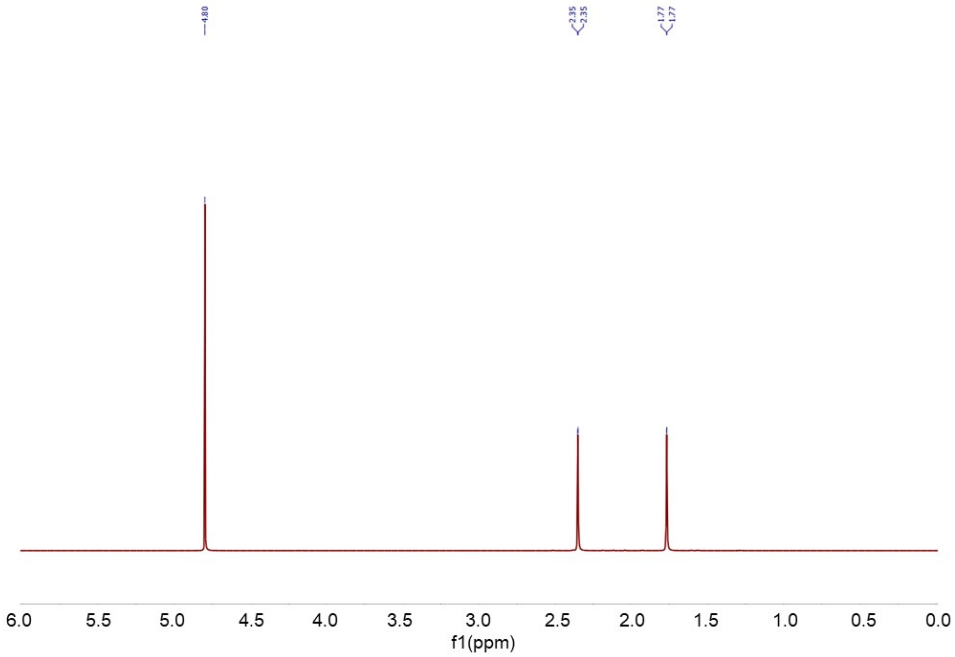

Figure S4. ^{1}H NMR spectra of *syn*-(Me,Me)bimane (D_2O, 400 MHz)

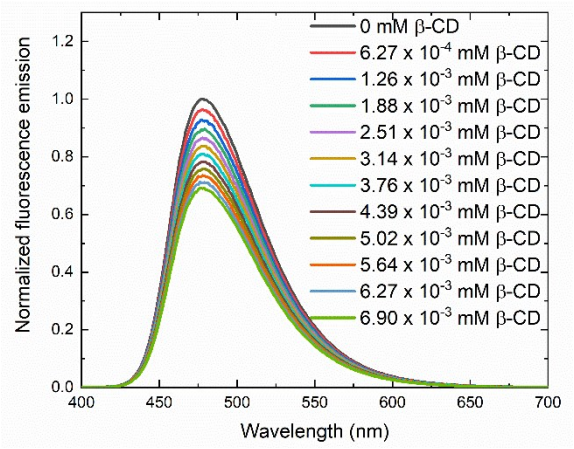

Figure S5. Changes in the bimane fluorescence emission as a function of increasing concentration of β-cyclodextrin. [Bimane] = 5.0 x 10^{-2} mM.

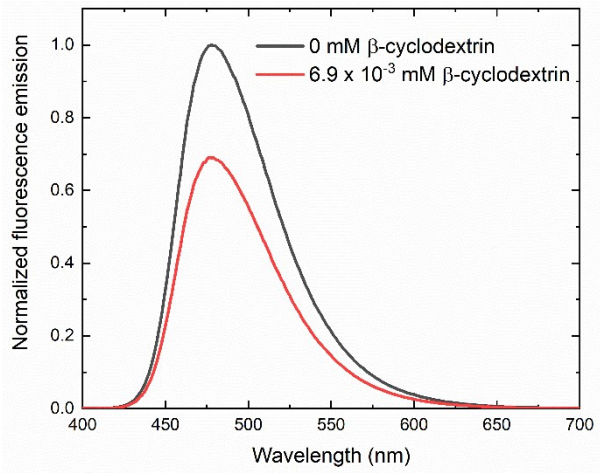

Figure S6. Summary of how changes in the concentration of β-cyclodextrin lead to a decrease in the fluorescence emission of bimane. [**1**] = 5.0 x 10^{-2} mM; $\lambda_{excitation}$ = 385 nm.

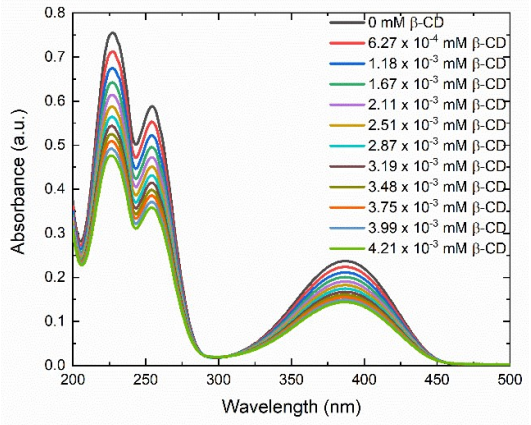

Figure S7. Changes in the bimane UV-visible absorption spectrum as a function of increasing concentration of β-cyclodextrin. [Bimane] = 5.0 x 10^{-2} mM.

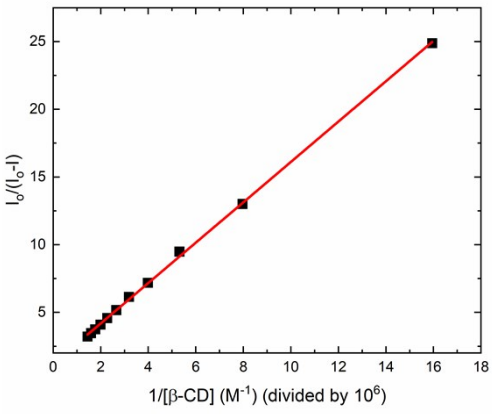

Figure S8. Benesi-Hildebrand plot illustrating the linear relationship between 1/[β-CD] on the X-axis and the change in fluorescence signal of the bimane ($I_o/(I_o-I)$ on the Y-axis. Equation: y = a + b*x; a = 1.19974; b = 1.49E-6; R^2 = 0.99943. [Bimane] = 5.0 x 10^{-2} mM.

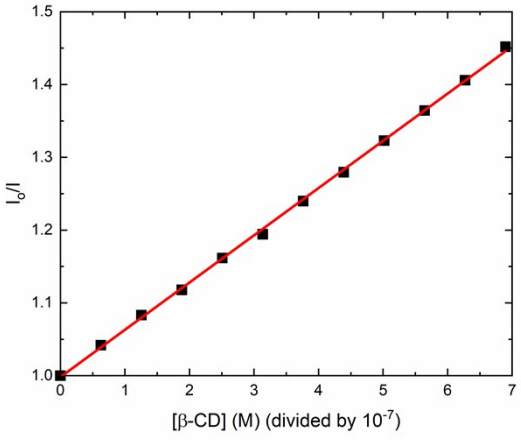

Figure S9. Stern-Volmer plot illustrating the linear relationship between [β-CD] on the X-axis and the ratio of initial emission divided by observed emission (*Io*/*I*) on the Y-axis. Equation: y = a + b*x; a = 0.99811; b = 648998; R^2 = 0.9994. [Bimane] = 5.0 x 10^{-2} mM.

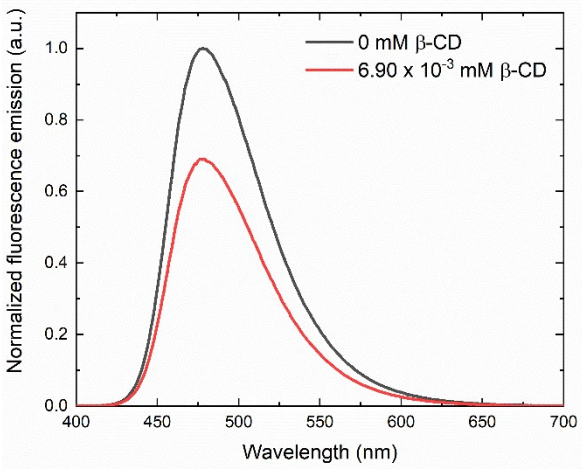

Figure S10. Summary of the changes in bimane fluorescence emission on going from 0 mM of β-cyclodextrin to 6.90 x 10^{-3} mM of β-cyclodextrin. [Bimane] = 5.0 x 10^{-2} mM.

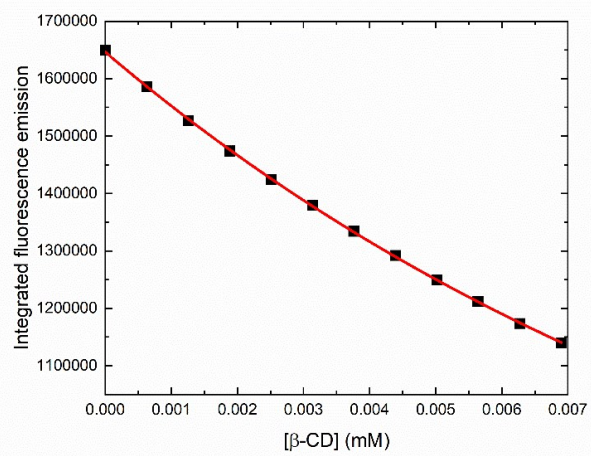

Figure S11. Normalized integrated emission of bimane in the presence of increasing concentrations of β-cyclodextrin, fit to a single exponential decay curve. [Bimane] = 5.0 x 10^{-2} mM. Equation: y = A1*exp(-x/t1)+B; y0 = 544722; A1 = 1101727; t1 = 0.01123; R^2 = 0.99989

SUMMARY FIGURES THAT ILLUSTRATE THE INTERACTION OF A VARIETY OF METAL SALTS WITH BIMANE

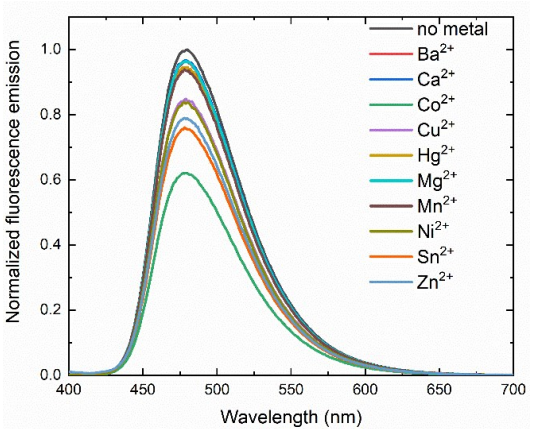

Figure S12. Summary of the fluorescence integration results from treating a solution of bimane **1** with a variety of metal chloride salts. [Bimane] = 5.0 x 10^{-2} mM; [metal salt] = 6.16 x 10^{-3} mM. All reported results represent an average of three trials.

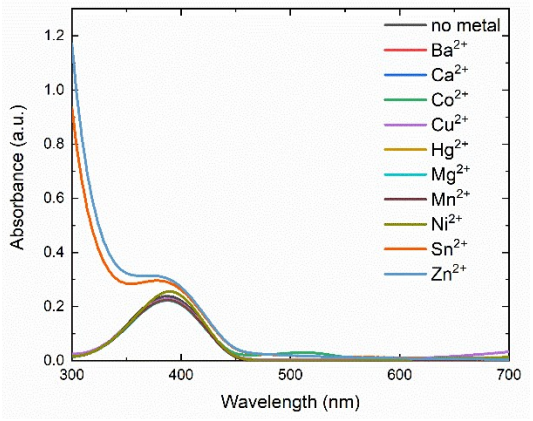

Figure S13. Summary of the UV-visible spectral changes from treating a solution of bimane **1** with a variety of metal chloride salts. [Bimane] = 5.0 x 10^{-2} mM; [metal salt] = 6.16 x 10^{-3} mM. All reported results represent an average of three trials.

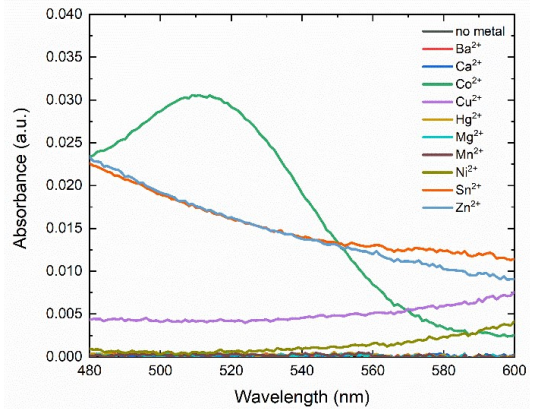

Figure S14. Zoomed-in view of the UV-visible spectral changes between 480 nm and 600 nm that occur from treating a solution of bimane **1** with a variety of metal chloride salts. [Bimane] = 5.0 x 10^{-2} mM; [metal salt] = 6.16 x 10^{-3} mM. All reported results represent an average of three trials.

SUMMARY FIGURES THAT ILLUSTRATE THE INTERACTION OF COBALT (II) CHLORIDE WITH BIMANE

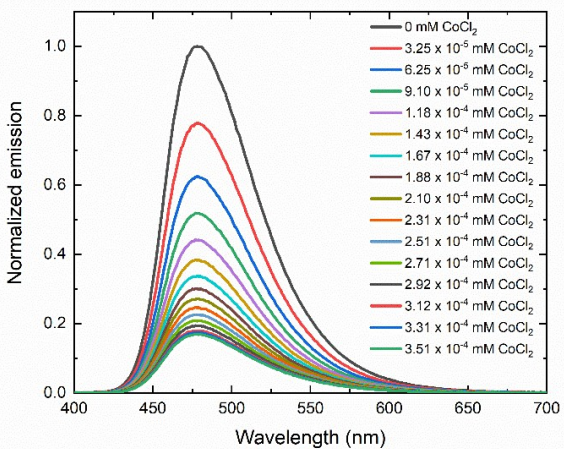

Figure S15. Normalized fluorescence spectra showing changes in the fluorescence emission of bimane as a function of changing concentrations of cobalt (II) chloride. [Bimane] = 5.0 x 10^{-2} mM.

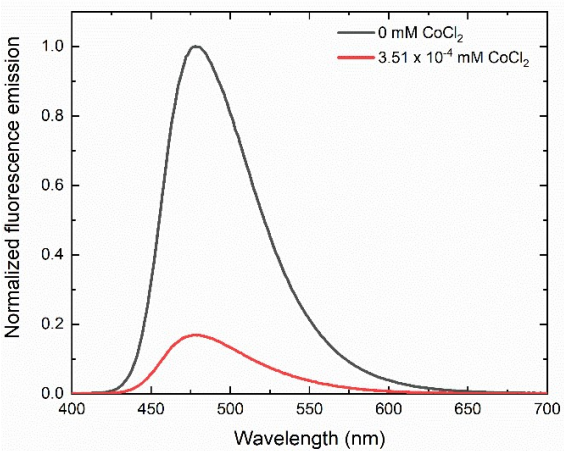

Figure S16. Summary of the changes in the bimane fluorescence emission spectra on going from 0 mM of cobalt (II) chloride to 3.31 x 10^{-4} mM of cobalt (II) chloride. [Bimane] = 5.0 x 10^{-2} mM

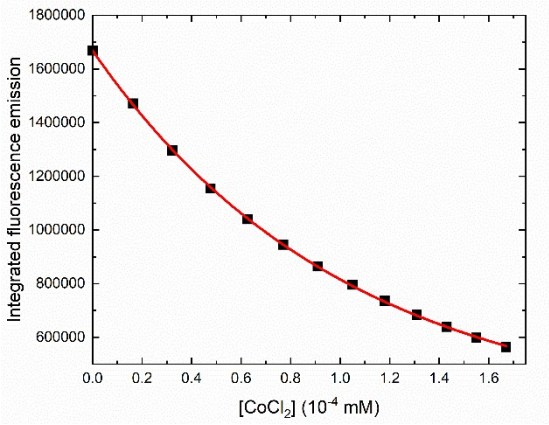

Figure S17. Normalized integrated emission of bimane in the presence of increasing concentrations of cobalt (II) chloride, fit to a single exponential decay curve. [Bimane] = 5.0 x 10^{-2} mM. Equation: y = A1*exp(-x/t1)+B; y0 = 299576; A1 = 1369368; t1 = 1.025E-4; R^2 = 0.9999

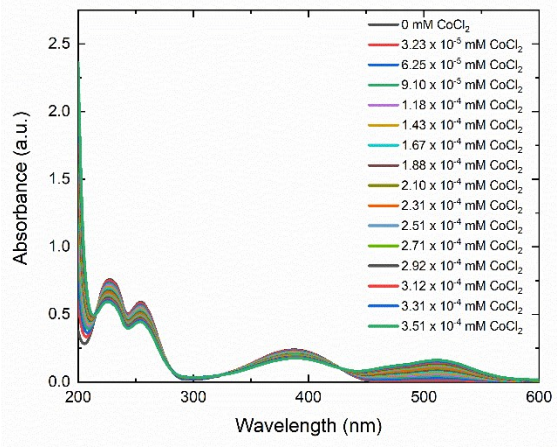

Figure S18. UV-visible absorption spectra showing changes in the absorbance of bimane as a function of increasing concentrations of cobalt (II) chloride. [Bimane] = 5.0 x 10^{-2} mM.

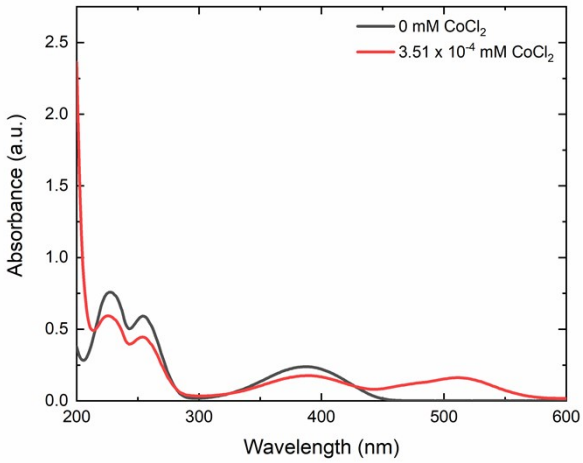

Figure S19. Summary of the changes in the bimane absorbance spectra on going from 0 mM of cobalt (II) chloride to 3.31 x 10^{-4} mM of cobalt (II) chloride. [Bimane] = 5.0 x 10^{-2} mM

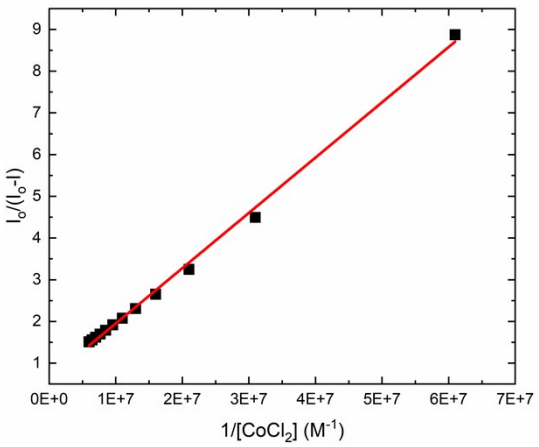

Figure S20. Benesi-Hildebrand plot illustrating the linear relationship between 1/[$CoCl_2$] on the X-axis and the change in fluorescence signal of the bimane (I_o/(I_o-I) on the Y-axis. Equation: y = a + b*x; a = 0.62491; b = 1.32547E-7; R^2 = 0.99702. [Bimane] = 5.0 x 10^{-2} mM.

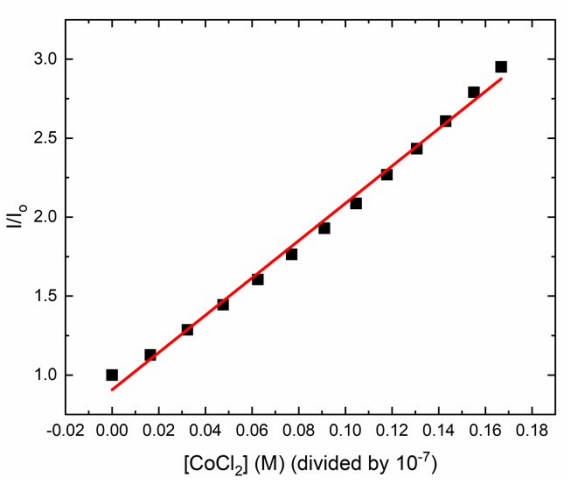

Figure S21. Stern-Volmer plot illustrating the linear relationship between [$CoCl_2$] on the X-axis and the ratio of initial emission divided by observed emission (*Io*/*I*) on the Y-axis. Equation: y = a + b*x; a = 0.90578; b = 1.18113E7; R^2 = 0. 99398. [Bimane] = 5.0 x 10^{-2} mM.

SUMMARY FIGURES THAT ILLUSTRATE THE INTERACTION OF COBALT (II) ACETATE WITH BIMANE

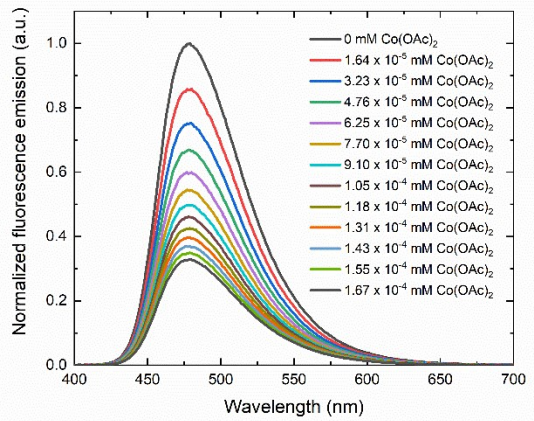

Figure S22. Changes in the bimane fluorescence emission as a function of increasing concentration of cobalt (II) acetate. [Bimane] = 5.0 x 10^{-2} mM.

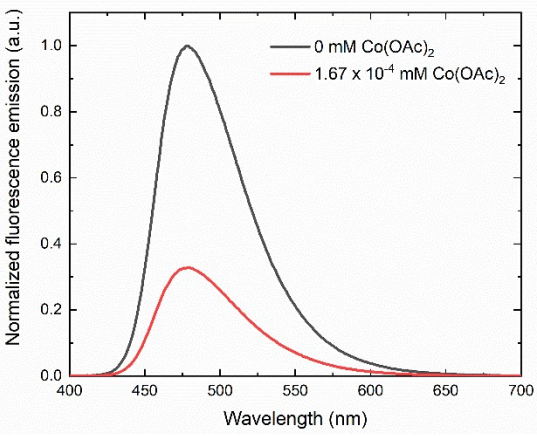

Figure S23. Summary of the changes in bimane fluorescence emission on going from 0 mM of cobalt (II) acetate to 1.67 x 10^{-4} mM of cobalt (II) acetate. [Bimane] = 5.0 x 10^{-2} mM.

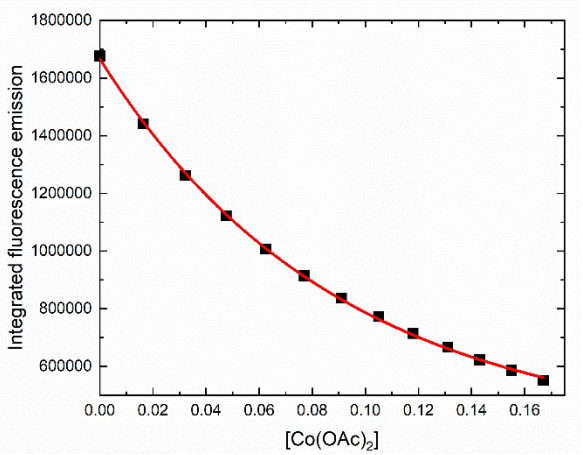

Figure S24. Normalized integrated emission of bimane in the presence of increasing concentrations of cobalt (II) acetate, fit to a single exponential decay curve. [Bimane] = 5.0 x 10^{-2} mM. Equation: y = A1*exp(-x/t1)+B; y0 = 358996; A1 = 1308012; t1 = 8.9459E-5; R^2 = 0.99964

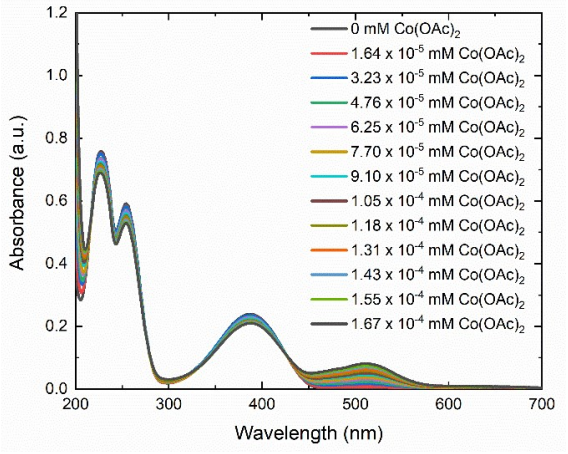

Figure S25. UV-visible absorption spectra showing changes in the absorbance of bimane as a function of increasing concentrations of cobalt (II) acetate. [Bimane] = 5.0 x 10^{-2} mM.

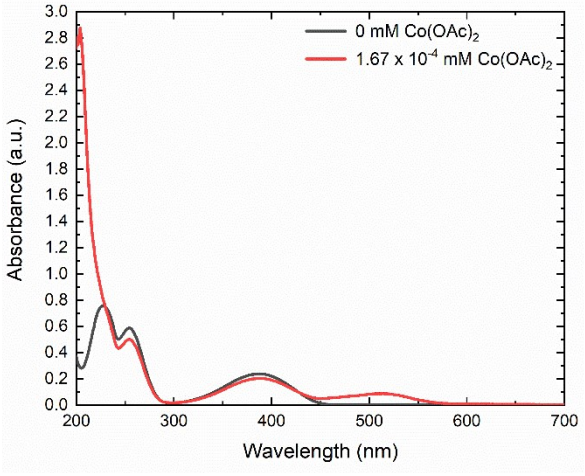

Figure S26. Summary of the changes in the bimane absorbance spectrum on going from 0 mM of cobalt (II) acetate to 1.67 x 10^{-4} mM of cobalt (II) acetate. [Bimane] = 5.0 x 10^{-2} mM

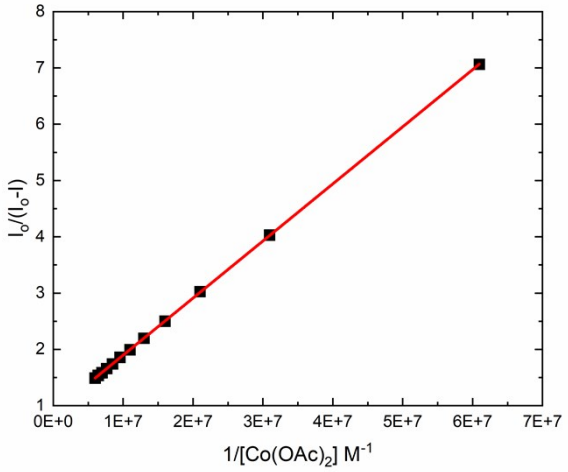

Figure S27. Benesi-Hildebrand plot illustrating the linear relationship between 1/[$Co(OAc)_2$] on the X-axis and the change in fluorescence signal of the bimane ($I_o/(I_o-I)$ on the Y-axis. Equation: y = a + b*x; a = 0.88169; b = 1.01449E-7; R^2 = 0.99999. [Bimane] = 5.0 x 10^{-2} mM.

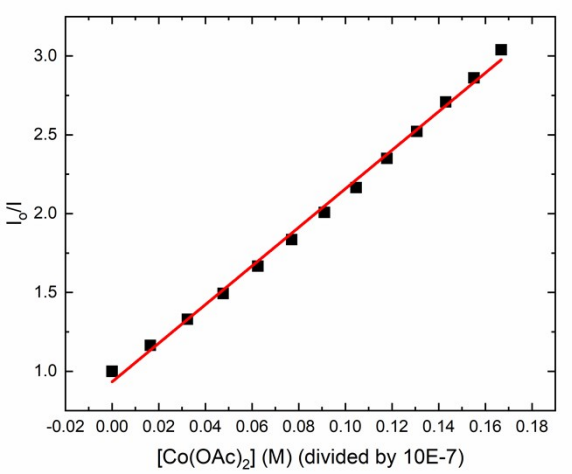

Figure S28. Stern-Volmer plot illustrating the linear relationship between $[Co(OAc)_2]$ on the X-axis and the ratio of initial emission divided by observed emission (*Io*/*I*) on the Y-axis. Equation: y = a + b*x; a = 0.93267; b = 1.22494E7; R^2 = 0.99646. [Bimane] = 5.0 x 10^{-2} mM.

SUMMARY FIGURES THAT ILLUSTRATE THE INTERACTION OF A VARIETY OF METAL SALTS WITH A BIMANE:β- CYCLODEXTRIN COMPLEX

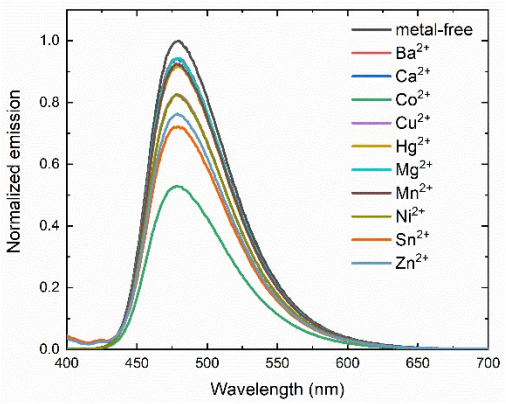

Figure S29. Summary of the fluorescence integration results from treating a solution of bimane **1** with a variety of metal chloride salts. [Bimane] = 5.0 x 10^{-2} mM; [metal salt] = 6.16 x 10^{-3} mM. All reported results represent an average of three trials.

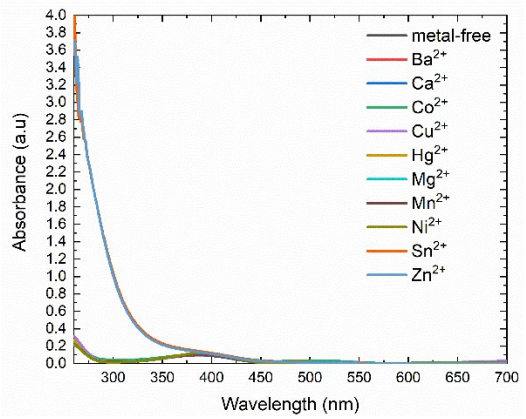

Figure S30. Summary of the UV-visible spectral changes from treating a solution of bimane **1** with a variety of metal chloride salts. [Bimane] = 5.0 x 10^{-2} mM; [metal salt] = 6.16 x 10^{-3} mM. All reported results represent an average of three trials.

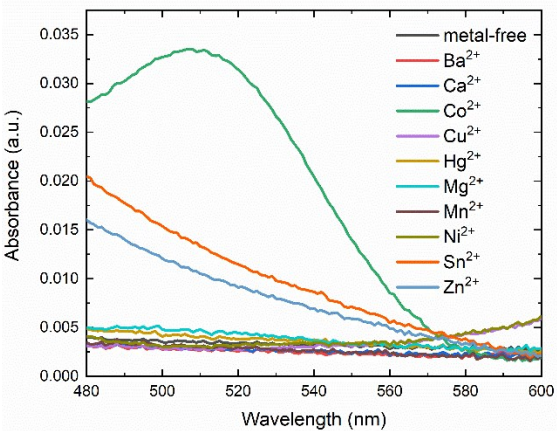

Figure S31. Zoomed-in view of the UV-visible spectral changes between 480 nm and 600 nm that occur from treating a solution of bimane **1** with a variety of metal chloride salts. [Bimane] = 5.0 x 10^{-2} mM; [metal salt] = 6.16 x 10^{-3} mM. All reported results represent an average of three trials.

SUMMARY FIGURES THAT ILLUSTRATE THE INTERACTION OF INCREASING CONCENTRATIONS OF COBALT (II) CHLORIDE WITH A BIMANE-β-CYCLODEXTRIN COMPLEX

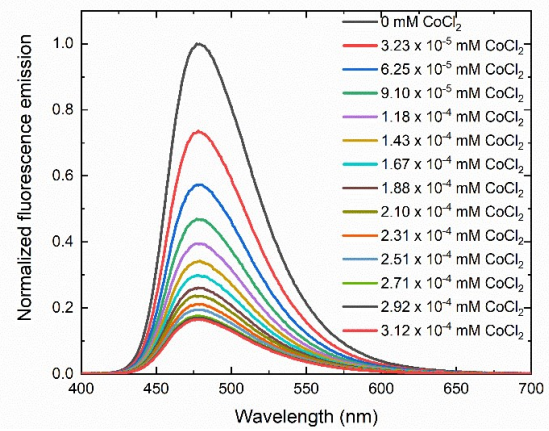

Figure S32. Normalized fluorescence spectra showing changes in the fluorescence emission of the bimane-β-cyclodextrin complex with increasing concentrations of cobalt (II) chloride. [Bimane] = 5.0 x 10^{-2} mM.

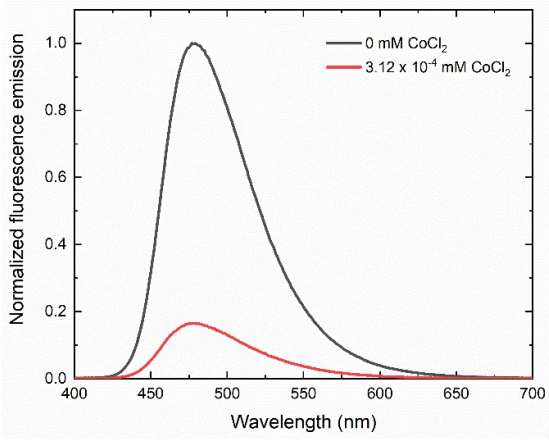

Figure S33. Summary of the changes in the bimane-β-cyclodextrin complex's fluorescence emission spectra on going from 0 mM of cobalt (II) chloride to 3.31 x 10^{-4} mM of cobalt (II) chloride. [Bimane] = 5.0 x 10^{-2} mM

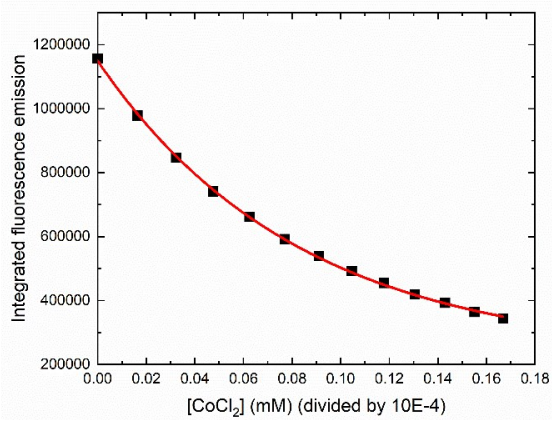

Figure S34. Normalized integrated emission of the bimane-β-cyclodextrin complex in the presence of increasing concentrations of cobalt (II) chloride, fit to a single exponential decay curve. [Bimane] = 5.0 x 10^{-2} mM. Equation: y = A1*exp(-x/t1)+B; y0 = 226160; A1 = 923507; t1 = 8.29584E-5; R^2 = 0.99962.

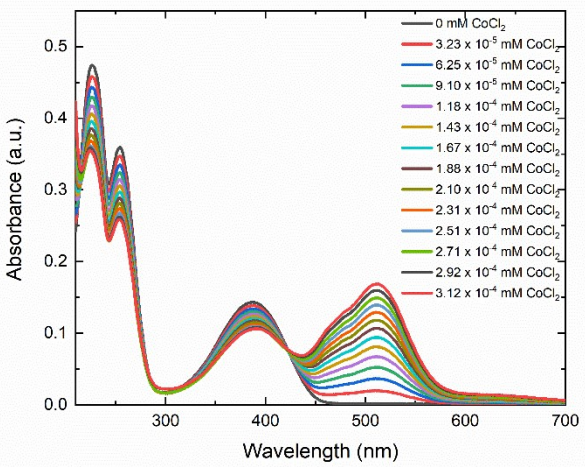

Figure S35. UV-visible absorption spectra showing changes in the absorbance of the bimane-β-cyclodextrin complex at increasing concentrations of cobalt (II) chloride. [Bimane] = 5.0 x 10^{-2} mM.

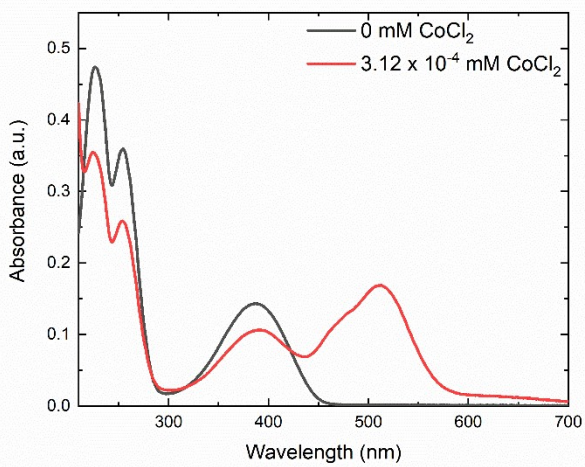

Figure S36. Summary of the changes in the bimane-β-cyclodextrin complex's absorbance spectra on going from 0 mM of cobalt (II) chloride to 3.31 x 10^{-4} mM of cobalt (II) chloride. [Bimane] = 5.0 x 10^{-2} mM

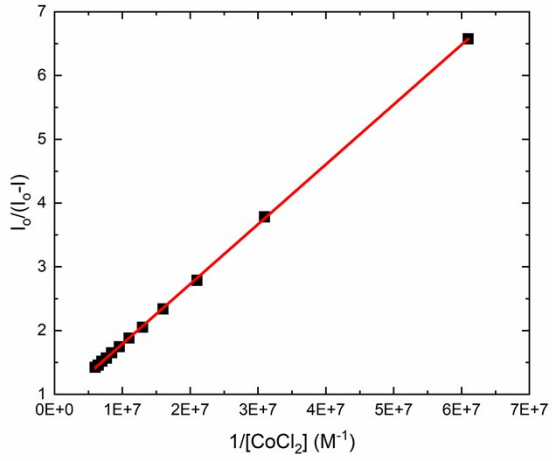

Figure S37. Benesi-Hildebrand plot illustrating the linear relationship between 1/[$CoCl_2$] on the X-axis and the change in fluorescence signal of the bimane-β-cyclodextrin complex ($I_o/(I_o-I)$ on the Y-axis. Equation: y = a + b*x; a = 0.85062; b = 9.38673E-8; R^2 = 0.99988. [Bimane] = 5.0 x 10^{-2} mM.

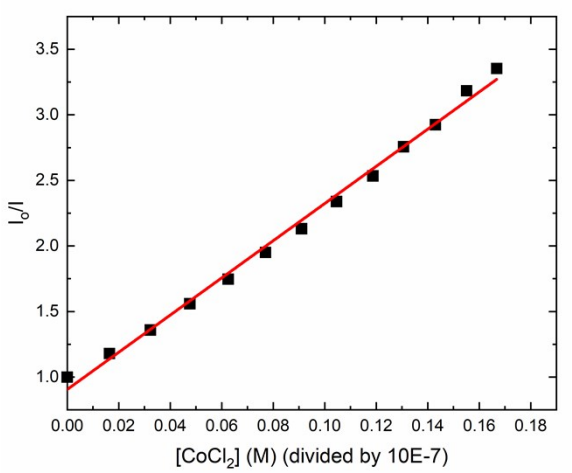

Figure S38. Stern-Volmer plot illustrating the linear relationship between [$CoCl_2$] on the X-axis and the ratio of initial emission divided by observed emission (*Io*/*I*) for the bimane-β-cyclodextrin complex on the Y-axis. Equation: y = a + b*x; a = 0.90546; b = 1.41813E7; R^2 = 0.99465. [Bimane] = 5.0 x 10^{-2} mM.

SUMMARY FIGURES THAT ILLUSTRATE THE INTERACTION OF INCREASING CONCENTRATIONS OF COBALT (II) ACETATE WITH A BIMANE-β-CYCLODEXTRIN COMPLEX

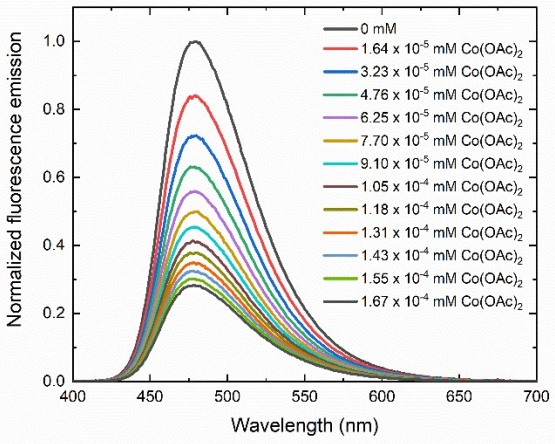

Figure S39. Changes in the bimane-β-cyclodextrin complex fluorescence emission as a function of increasing concentration of cobalt (II) acetate. [Bimane] = 5.0 x 10^{-2} mM.

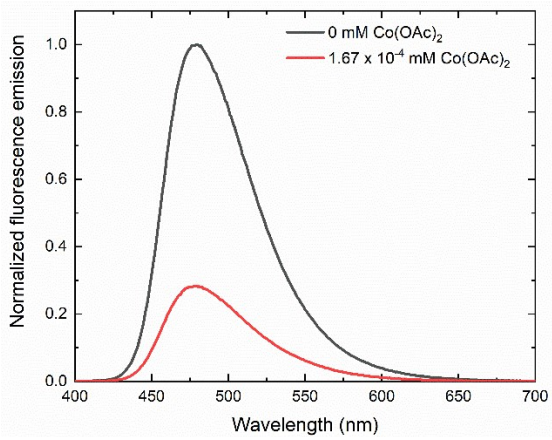

Figure S40. Summary of the changes in bimane-β-cyclodextrin complex fluorescence emission on going from 0 mM of cobalt (II) acetate to 1.67 x 10^{-4} mM of cobalt (II) acetate. [Bimane] = 5.0 x 10^{-2} mM.

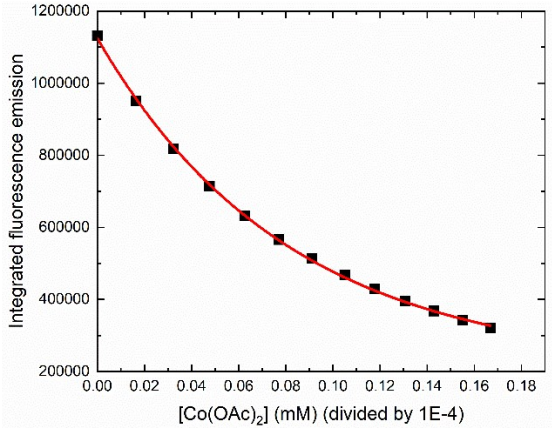

Figure S41. Normalized integrated emission of the bimane-β-cyclodextrin complex in the presence of increasing concentrations of cobalt (II) acetate, fit to a single exponential decay curve. [Bimane] = 5.0 x 10^{-2} mM. Equation: y = A1*exp(-x/t1)+B; y0 = 210333; A1 = 914383; t1 = 8.11467E-5; R^2 = 0.9996.

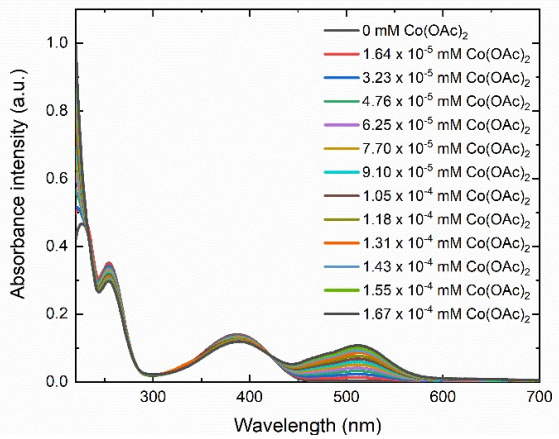

Figure S42. UV-visible absorption spectra showing changes in the absorbance of the bimane-β-cyclodextrin complex as a function of increasing concentrations of cobalt (II) acetate. [Bimane] = 5.0 x 10^{-2} mM.

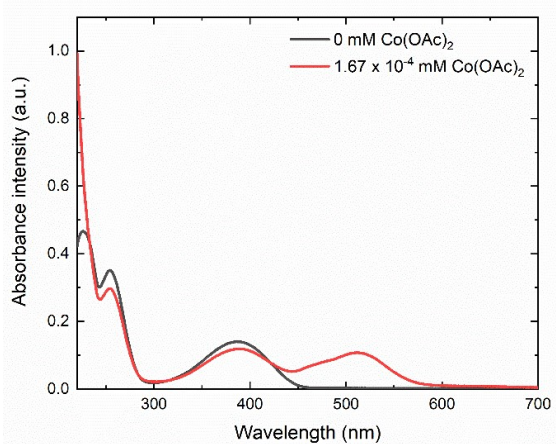

Figure S43. Summary of the changes in the bimane-β-cyclodextrin complex absorbance spectrum on going from 0 mM of cobalt (II) acetate to 1.67 x 10^{-4} mM of cobalt (II) acetate. [Bimane] = 5.0 x 10^{-2} mM

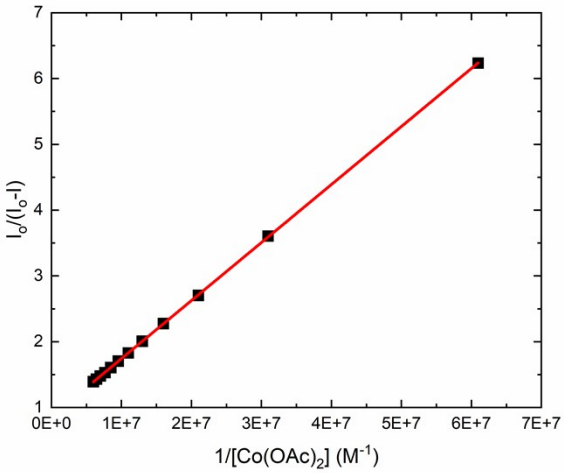

Figure S44. Benesi-Hildebrand plot illustrating the linear relationship between 1/[$Co(OAc)_2$] on the X-axis and the change in fluorescence signal of the bimane-β-cyclodextrin complex ($I_o/(I_o-I)$ on the Y-axis. Equation: y = a + b*x; a = 0.86075; b = 8.81923E-8; R^2 = 0.99998. [Bimane] = 5.0 x 10^{-2} mM.

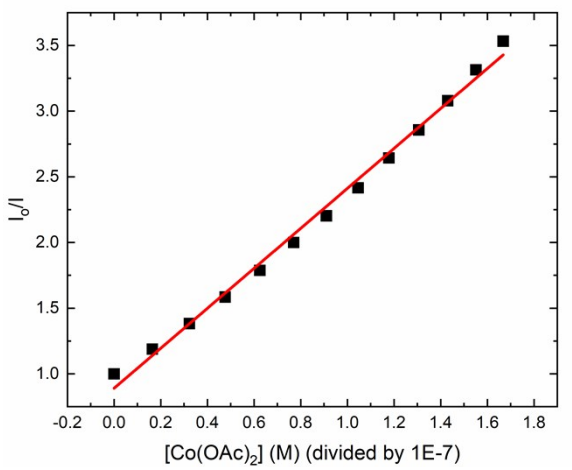

Figure S45. Stern-Volmer plot illustrating the linear relationship between $[Co(OAc)_2]$ on the X-axis and the ratio of initial emission divided by observed emission (*Io*/*I*) for the bimane-β-cyclodextrin complex on the Y-axis. Equation: y = a + b*x; a = 0.89005; b = 1.52145E7; R^2 = 0.99404. [Bimane] = 5.0 x 10^{-2} mM.

SUMMARY FIGURES ILLUSTRATING EXPERIMENTS IN TAP WATER

Bimane response to cobalt (II) chloride in tap water

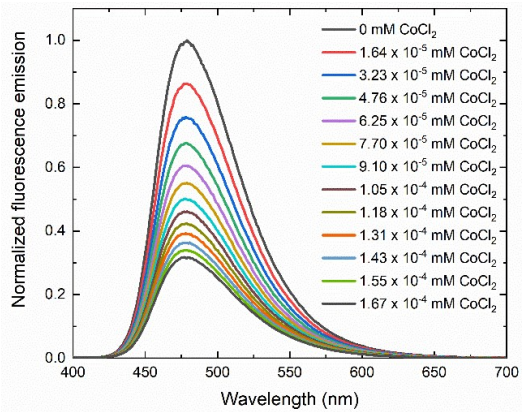

Figure S46. Changes in the bimane fluorescence emission as a function of increasing concentration of cobalt chloride in tap water. [Bimane] = 5.0 x 10^{-2} mM.

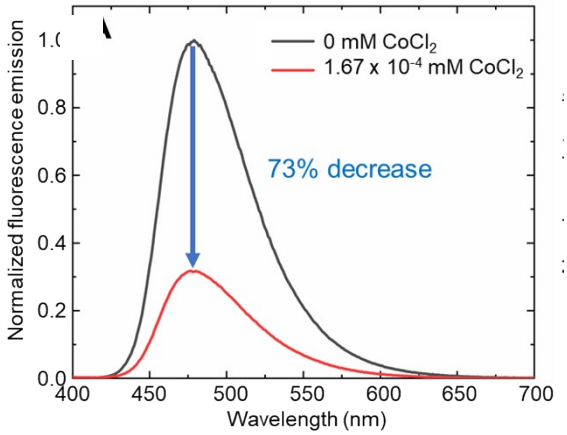

Figure S47. Summary of the changes in the bimane fluorescence emission as a function of increasing concentration of cobalt chloride in tap water. [Bimane] = 5.0 x 10^{-2} mM.

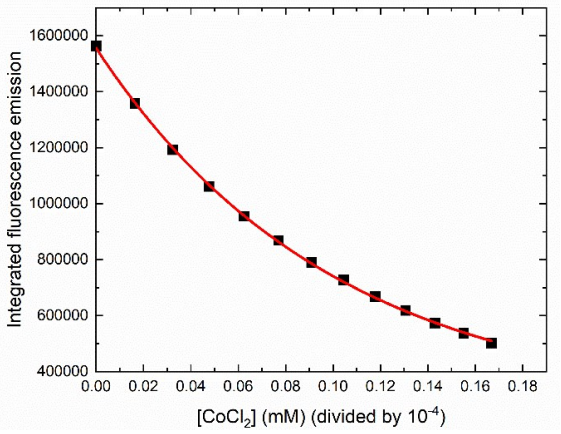

Figure S48. Normalized integrated emission of bimane in the presence of increasing concentrations of cobalt chloride in tap water, fit to a single exponential decay curve. [Bimane] = 5.0 x 10^{-2} mM. Equation: y = A1*exp(-x/t1)+B; y0 = 265558; A1 = 1290590; t1 = 1.00174E-4; R^2 = 0.99974.

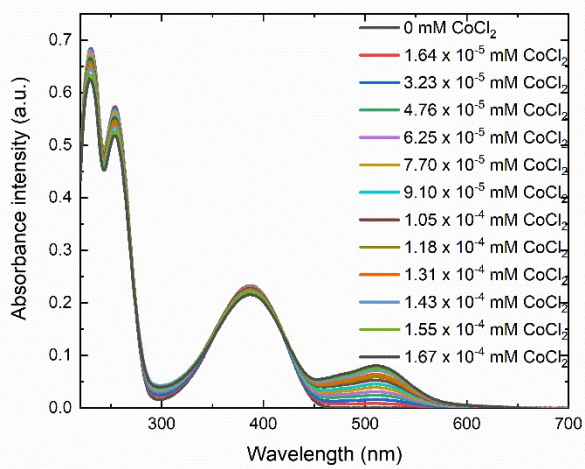

Figure S49. UV-visible absorption spectra showing changes in the absorbance of bimane as a function of increasing concentrations of cobalt chloride in tap water. [Bimane] = 5.0 x 10^{-2} mM.

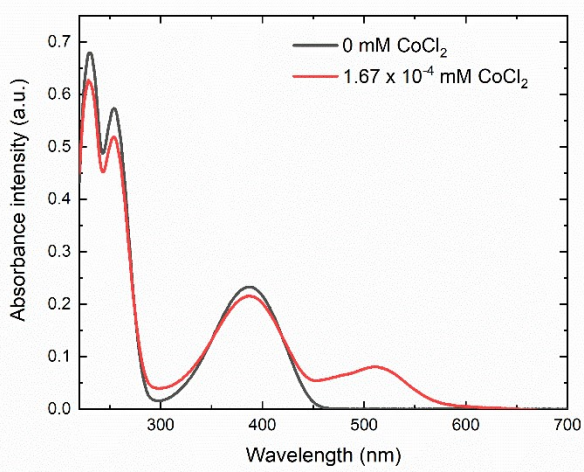

Figure S50. Summary of the changes in the bimane absorbance spectrum on going from 0 mM of cobalt chloride to 1.67 x 10^{-4} mM of cobalt chloride in tap water. [Bimane] = 5.0 x 10^{-2} mM

Response of the bimane:β- cyclodextrin complex to cobalt (II) chloride in tap water

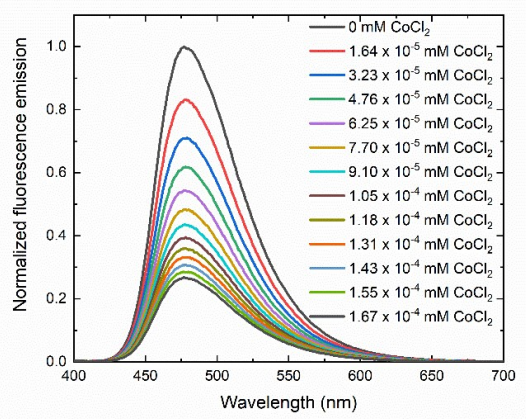

Figure S51. Changes in the fluorescence emission of the bimane: β-cyclodextrin complex as a function of increasing concentration of cobalt chloride in tap water. [Bimane] = 5.0 x 10^{-2} mM.

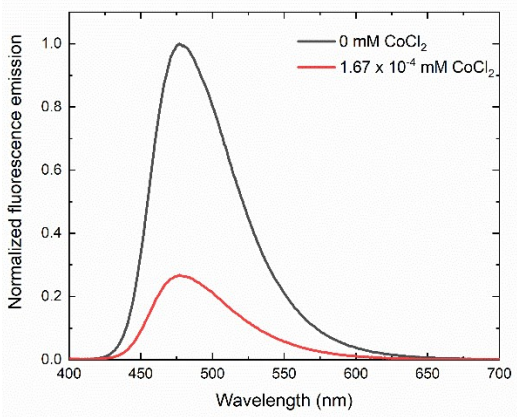

Figure S52. Summary of the changes in the fluorescence emission of the bimane: β-cyclodextrin complex as a function of increasing concentration of cobalt chloride in tap water. [Bimane] = 5.0 x 10^{-2} mM.

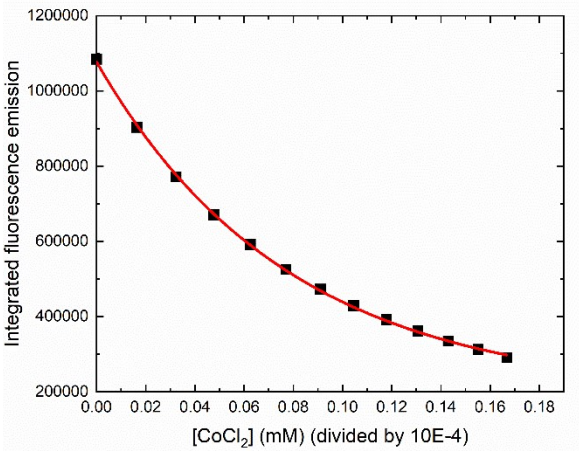

Figure S53. Normalized integrated emission of the bimane: β-cyclodextrin complex in the presence of increasing concentrations of cobalt chloride in tap water, fit to a single exponential decay curve. [Bimane] = 5.0 x 10^{-2} mM. Equation: y = A1*exp(-x/t1)+B; y0 = 193736; A1 = 883429; t1 = 7.80091E-5; R^2 = 0.99963.

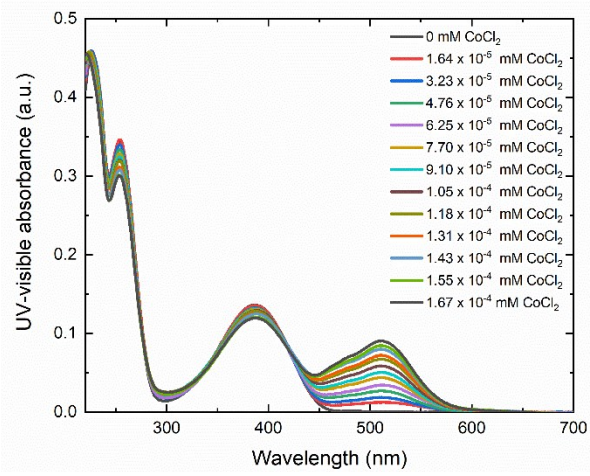

Figure S54. UV-visible absorption spectra showing changes in the absorbance of the bimane: β-cyclodextrin complex as a function of increasing concentrations of cobalt chloride in tap water. [Bimane] = 5.0 x 10^{-2} mM.

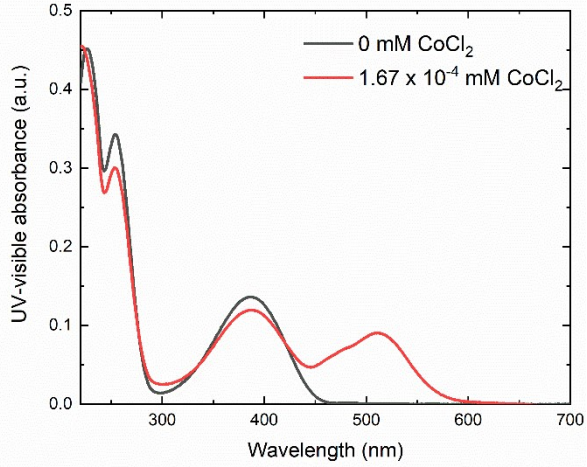

Figure S55. Summary of the changes in the absorbance of the bimane: β-cyclodextrin complex on going from 0 mM of cobalt chloride to 1.67 x 10^{-4} mM of cobalt chloride in tap water. [Bimane] = 5.0 x 10^{-2} mM

SUMMARY FIGURES ILLUSTRATING SOLID-STATE FTIR SPECTROSCOPY RESULTS

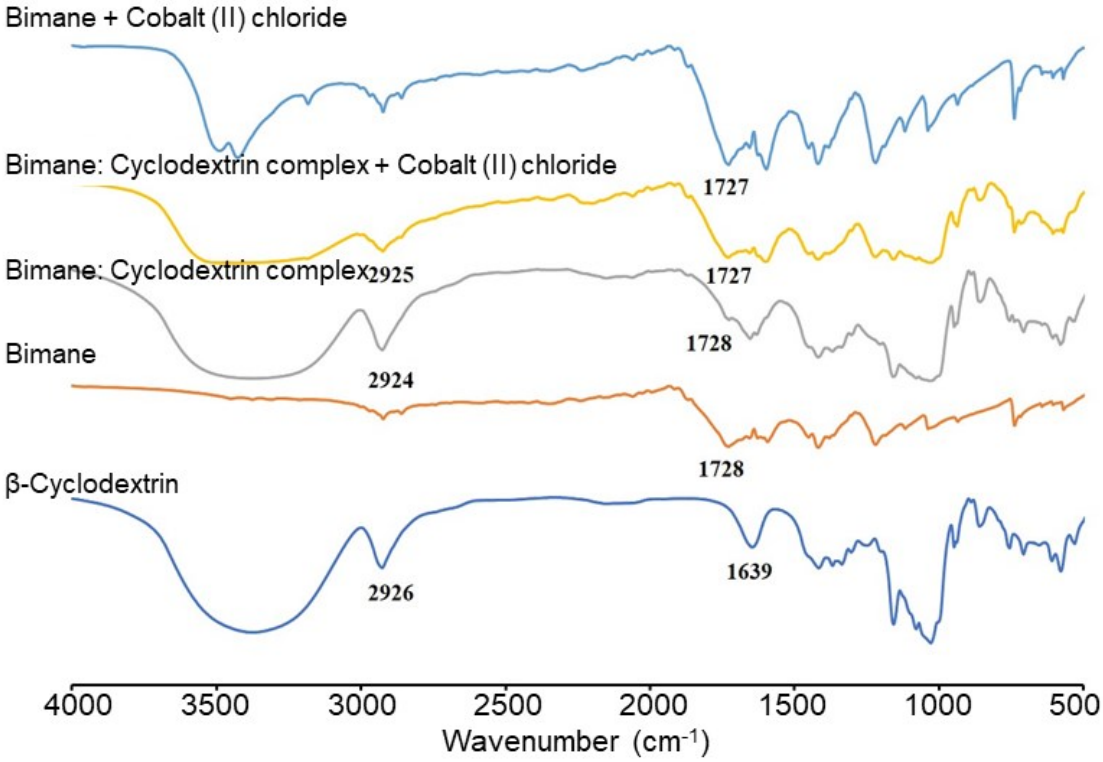

Figure S56. Illustration of solid-state FTIR spectroscopy results for a β-cyclodextrin sample, a bimane sample the complex of bimane in β-cyclodextrin, and the samples after the addition of cobalt (II) chloride to the bimane: β-cyclodextrin complex and to bimane alone

SUMMARY FIGURES ILLUSTRATING THE APPEARANCE OF FUNCTIONALIZED PAPER STRIPS UNDER UV-LIGHT IRRADIATION.

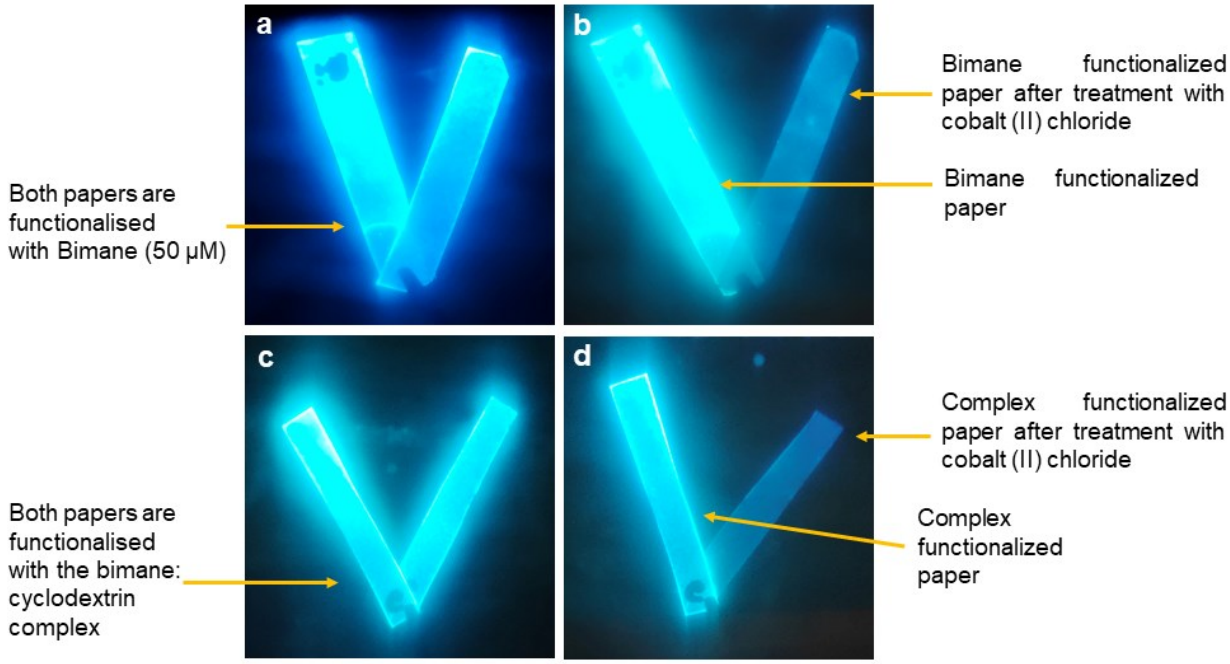

Figure S57. Illustration of how functionalized paper changes its appearance under UV-light irradiation in the presence of cobalt (II) chloride. (a) Both papers are functionalized with a 50.0 µM solution of bimane; (b) the left paper is functionalized with a 50.0 µM solution of bimane and the right paper is functionalized with the same concentration of bimane but was subsequently exposed to a 200 µL of 0.1 M solution of cobalt (II) chloride; (c) both papers are functionalized with a solution of the bimane: β-cyclodextrin (50.0 µM bimane in 56.5 µM β-cyclodextrin) complex; (d) the left paper is functionalized with a solution of the bimane: β-cyclodextrin complex and the right paper is functionalized with the same concentration of complex but was subsequently exposed to a 200 µL of 0.1 M solution of cobalt (II) chloride

SUMMARY FIGURES ILLUSTRATING CHANGES IN SOLUTION COLOR IN THE PRESENCE OF VARIOUS METAL ADDITIVES

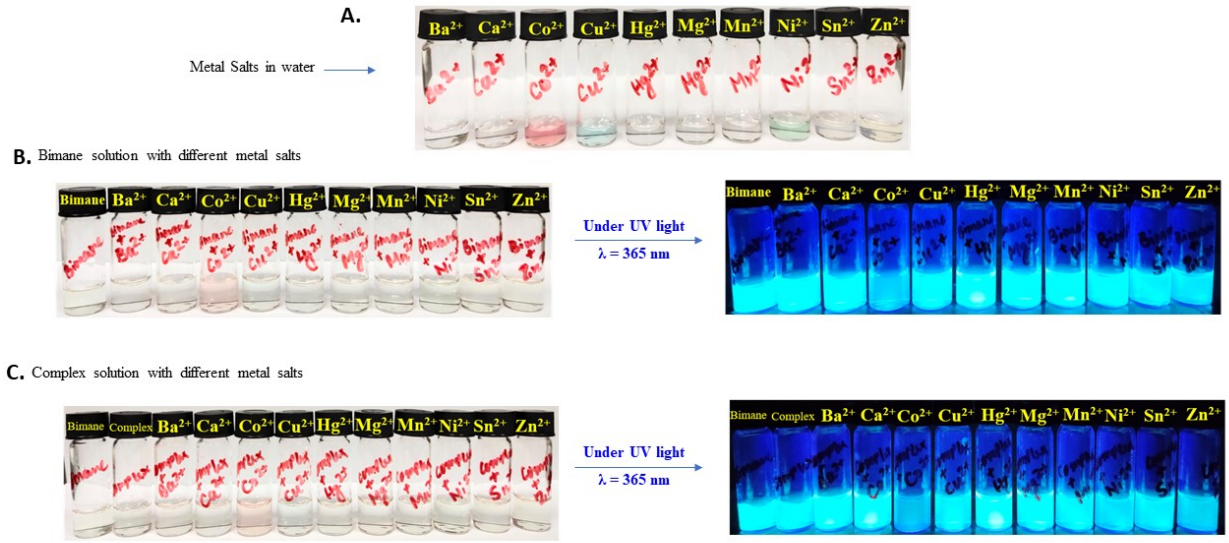

Figure S58. Illustration of the colorimetric and fluorometric responses of solutions to the presence of cobalt (II) chloride. (A) A photograph of 0.5 mL of various metal salts (0.1 M) in water under ambient lighting conditions; (B) a photograph of 1 mL of the bimane solutions (50.0 μM) in the presence of metal additives (200 μL of 0.1 M) under ambient lighting conditions, as well as a photograph of the same solutions under 365 nm ultraviolet light irradiation; (C) a photograph of 1 mL of the bimane: β-cyclodextrin complex (50.0 μM bimane in 56.5 μM β-CD) in the presence of various metal additives (200 μL of 0.1 M) under ambient lighting conditions, as well as a photograph of the same solutions under 365 nm ultraviolet light irradiation

SUMMARY FIGURES FOR LIMIT OF DETECTION STUDIES

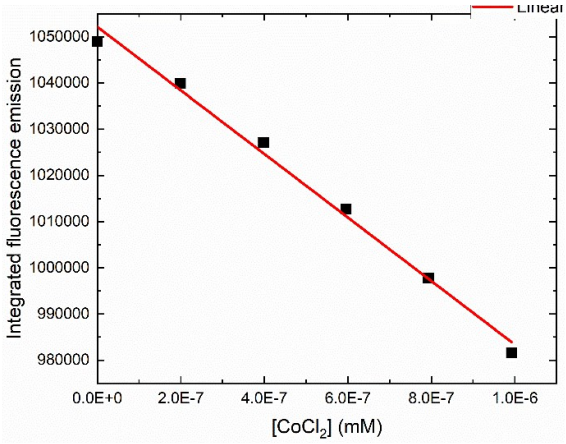

Figure S59. Calibration curve summarizing the relationship between the concentration of cobalt (II) chloride in double distilled water on the X-axis and integrated emission of bimane on the Y-axis. Y = (-7E10)x + (1E6); $R^2 = 0.9922$.

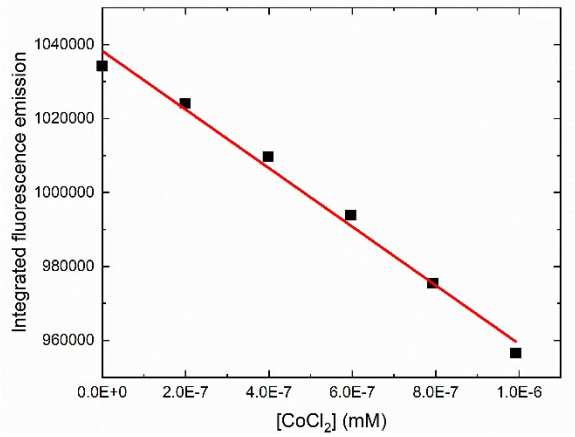

Figure S60. Calibration curve summarizing the relationship between the concentration of cobalt (II) chloride in double distilled water on the X-axis and integrated emission of the bimane: β-cyclodextrin complex on the Y-axis. Y = (-8E10)x + (1E6); $R^2 = 0.9896$.

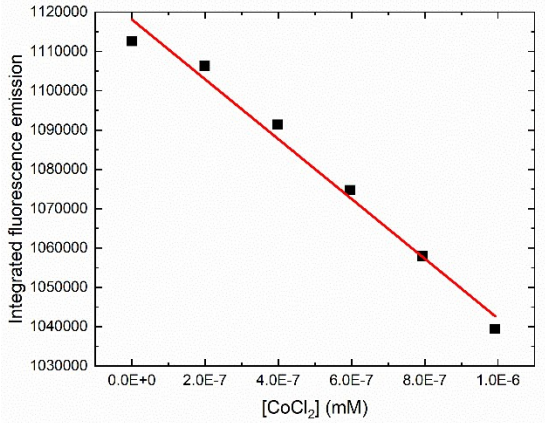

Figure S61. Calibration curve summarizing the relationship between the concentration of cobalt (II) chloride in tap water on the X-axis and integrated emission of bimane on the Y-axis. Y = (-8E10)x + (1E6); $R^2 = 0.9832$.

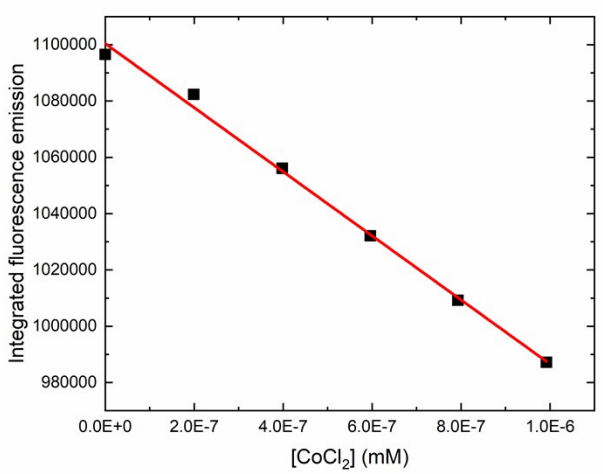

Figure S62. Calibration curve summarizing the relationship between the concentration of cobalt (II) chloride in tap water on the X-axis and integrated emission of the bimane: β-cyclodextrin complex on the Y-axis. $Y = (-1E11)x + (1E6)$; $R^2 = 0.9957$.

SUMMARY FIGURES FOR ^{1}H NMR TITRATION STUDIES

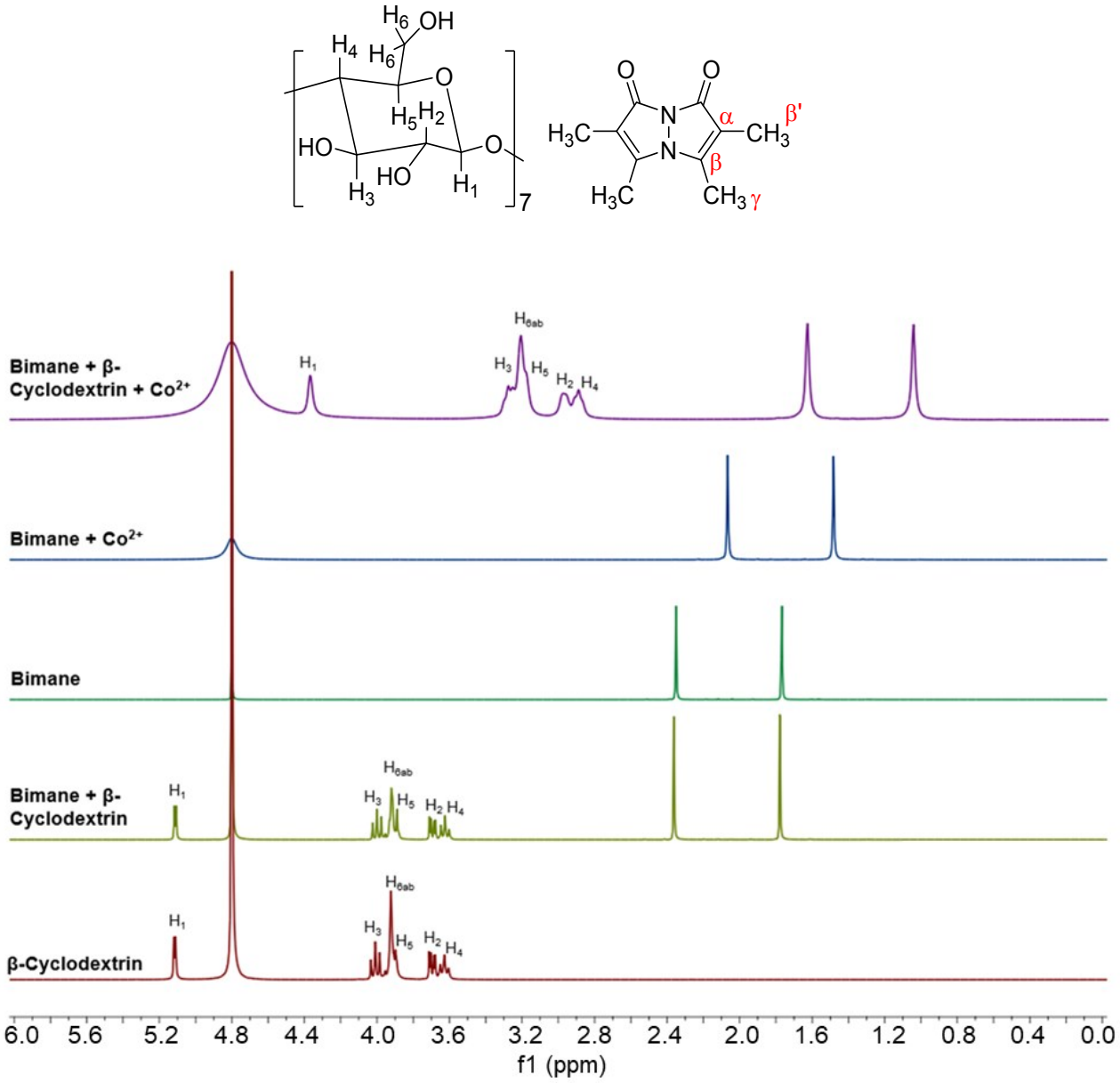

Figure S63. Illustration of ^{1}H NMR spectroscopy results for a β-cyclodextrin sample, a bimane sample, the complex of bimane in β-cyclodextrin, and the samples after the addition of cobalt (II) chloride to the bimane: β-cyclodextrin complex and to bimane alone

Summary Figures for Relative Quantum Yield Studies

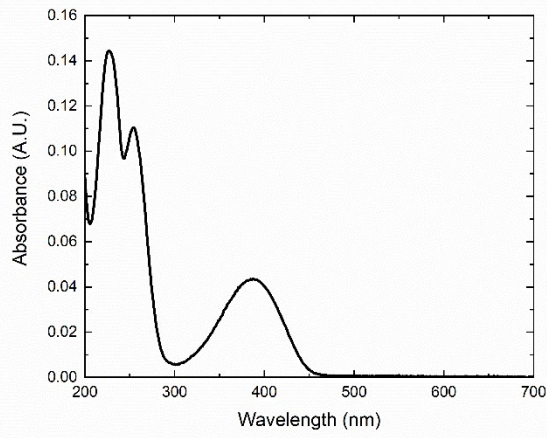

Figure S64. UV-Visible absorption spectrum of bimane **1** in water used for relative quantum yield calculations

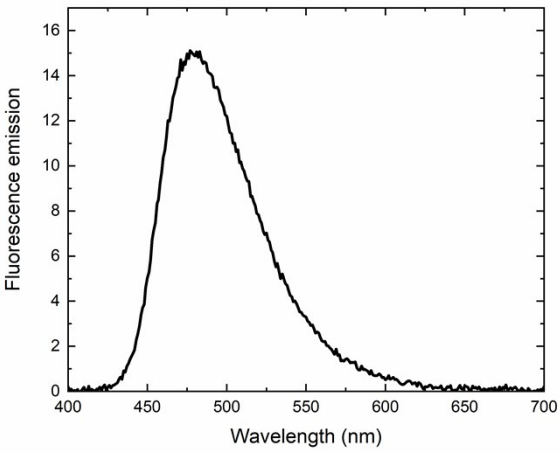

Figure S65. Fluorescence emission spectrum of bimane **1** in water used for relative quantum yield calculations

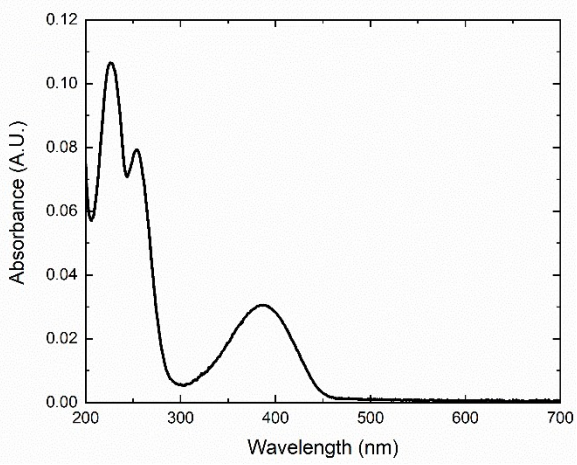

Figure S66. UV-Visible absorption spectrum of bimane **1** in a complex with β-cyclodextrin in water used for relative quantum yield calculations

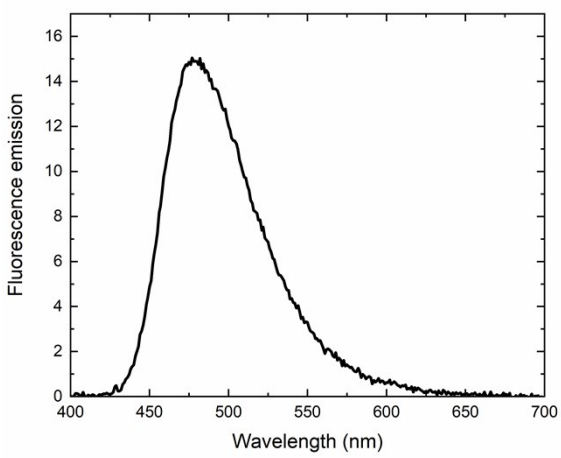

Figure S67. Fluorescence emission spectrum of bimane **1** in a complex with β-cyclodextrin in water used for relative quantum yield calculations

Summary Figures for Metal Competition Studies to Determine Cobalt Selectivity

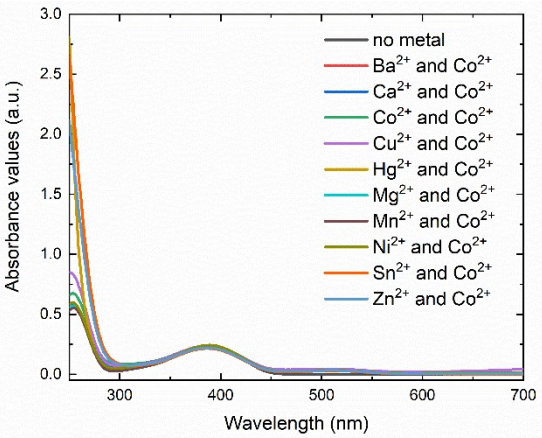

Figure S67. UV-visible spectra of bimane **1** in the presence of cobalt (II) chloride as well as cobalt (II) chloride mixed with other metals

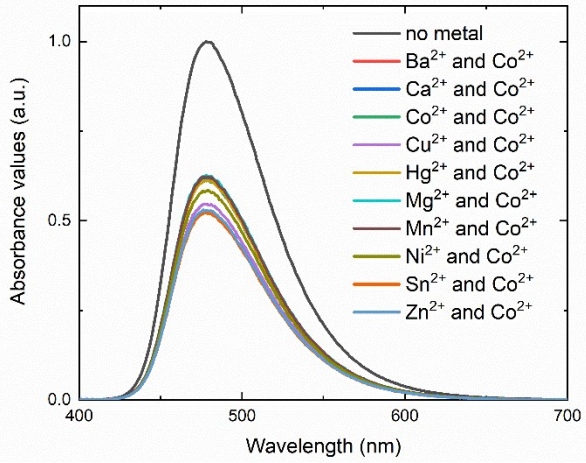

Figure S68. Fluorescence emission spectra of bimane **1** in the presence of cobalt (II) chloride as well as cobalt (II) chloride mixed with other metals

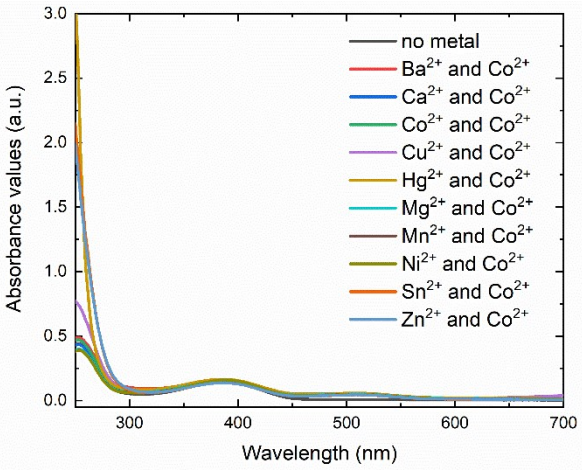

Figure S69. UV-visible spectra of a complex of bimane **1** with β-cyclodextrin in the presence of cobalt (II) chloride as well as cobalt (II) chloride mixed with other metals

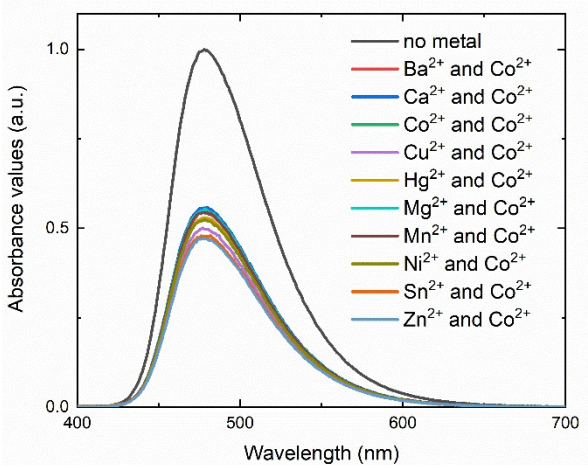

Figure S70. Fluorescence emission spectra a complex of bimane **1** with β-cyclodextrin in the presence of cobalt (II) chloride as well as cobalt (II) chloride mixed with other metals

REFERENCES

1 I. Neogi, P. J. Das, F. Grynszpan, *Synlett,* 2018, **29**, 1043-1046.

2 E. M. Kosower, B. Pazhenchevsky, *J. Am. Chem. Soc*., 1980, **102**, 4983-4993.

[3] Lakowicz, J. *Principles of Fluorescence Spectroscopy*, Third edition.; Springer: New york USA, 2006.

[4] Brouwer, A. M. Standards for Photoluminescence Quantum Yield Measurements in Solution (IUPAC Technical Report). *Pure Appl. Chem.* **2011**, *83* (12), 2213–2228.

[5] Kosower, E. M.; Giniger, R.; Radkowsky, A.; Hebel, D.; Shusterman, A. *J. Phys. Chem.* **1986**, *90*, 5552-5557.